

# Magnetic degeneracy and hidden metallicity of the spin-density-wave state in ferropnictides

I. Eremin<sup>1,2,\*</sup> and A. V. Chubukov<sup>3</sup><sup>1</sup>Max-Planck-Institut für Physik Komplexer Systeme, D-01187 Dresden, Germany<sup>2</sup>Institute für Mathematische und Theoretische Physik, TU Braunschweig, 38106 Braunschweig, Germany<sup>3</sup>Department of Physics, University of Wisconsin–Madison, Madison, Wisconsin 53706, USA

(Received 8 November 2009; revised manuscript received 11 December 2009; published 13 January 2010)

We analyze spin-density-wave (SDW) order in iron-based superconductors and electronic structure in the SDW phase. We consider an itinerant model for Fe pnictides with two hole bands centered at  $(0,0)$  and two electron bands centered at  $(0,\pi)$  and  $(\pi,0)$  in the unfolded Brillouin zone. A SDW order in such a model is generally a combination of two components with momenta  $(0,\pi)$  and  $(\pi,0)$ , both yield  $(\pi,\pi)$  order in the folded zone. Neutron experiments, however, indicate that only one component is present. We show that  $(0,\pi)$  or  $(\pi,0)$  order is selected if we assume that only one hole band is involved in the SDW mixing with electron bands. A SDW order in such three-band model is highly degenerate for a perfect nesting and hole-electron interaction only but we show that ellipticity of electron pockets and interactions between electron bands break the degeneracy and favor the desired  $(0,\pi)$  or  $(\pi,0)$  order. We further show that stripe-ordered system remains a metal for arbitrary coupling. We analyze electronic structure for parameters relevant to the pnictides and argue that the resulting electronic structure is in good agreement with angle-resolved photoemission experiments. We discuss the differences between our model and  $J_1$ - $J_2$  model of localized spins.

DOI: 10.1103/PhysRevB.81.024511

PACS number(s): 75.30.Fv, 74.25.Jb, 74.70.Xa

## I. INTRODUCTION

The discovery of superconductivity in the oxypnictide LaFeAsO (Ref. 1) created a new class of Fe-based high- $T_c$  superconductors—ferropnictides (FPs). The phase diagram of FPs is similar to that of high- $T_c$  cuprates and contains an antiferromagnetic phase at small dopings and superconducting phase at larger dopings. There are two important distinctions, however. First, parent compounds of FPs are antiferromagnetic metals, and second, the pairing symmetry in FPs is, most likely, an extended  $s$  wave, with or without nodes.<sup>2,3</sup> Electronic structure of parent FPs in the normal state has been measured by angle-resolved photoemission (ARPES) (Ref. 4) and by magneto-oscillations.<sup>5</sup> It consists of two quasi-two-dimensional (quasi-2D) near-circular hole pockets of nonequal size, centered around  $\Gamma$  point  $(0,0)$ , and two quasi-2D elliptic electron pockets centered around  $(0,\pm\pi)$  and  $(\pm\pi,0)$  points in the unfolded Brillouin zone (BZ) which includes only Fe atoms. For tetragonal symmetry, the two electron pockets transform into each other under the rotation by  $90^\circ$ . In the folded BZ, which is used for experimental measurements because of two nonequivalent As positions with respect to an Fe plane, both electron pockets are centered around  $(\pi,\pi)$ . The dispersions near electron pockets and near hole pockets are reasonably close to each other apart from the sign change, i.e., there is a substantial degree of nesting between hole and electron bands. There also exists the fifth hole band near  $(\pi,\pi)$  but it is more three dimensional (3D) and does not seem to play a significant role, at least for spin-density-wave (SDW) magnetism.

In this paper we analyze spin and electronic structures of a magnetically ordered state in parent FPs below  $T_{\text{SDW}} \sim 150$  K.<sup>1,6,7</sup> We will only focus on FeAs materials. Neutron scattering measurements on parent FeAs pnictides have found that the ordered momentum in the unfolded BZ is either  $(0,\pi)$  or  $(\pi,0)$ , i.e., magnetic order consists of ferro-

magnetic stripes along one crystallographic direction in an Fe plane and antiferromagnetic stripes along the other direction.

Such magnetic order emerges in the  $J_1$ - $J_2$  model of localized spins with interactions between nearest and next-nearest neighbors ( $J_1$  and  $J_2$ , respectively), for  $J_2 > 0.5J_1$ .<sup>8,9</sup> A localized spin model, however, is best suitable for an insulator and is generally not applicable to a metal unless the system is close to a metal-insulator transition.<sup>9</sup> An alternative scenario, which we explore here, assumes that parent FeAs FPs are “good metals” made of itinerant electrons, and antiferromagnetic order is of SDW type. Given the electronic structure of FPs, it is natural to assume that SDW order emerges, at least partly, due to near nesting between the dispersions of holes and electrons.<sup>10–17</sup> Such nesting is known to give rise to magnetism in Cr (Ref. 18). The itinerant scenario for FPs is largely supported by a reasonable agreement between *ab initio* electronic-structure calculations<sup>19</sup> and magneto-oscillation and ARPES experiments,<sup>5,20–23</sup> although electronic-structure calculations also indicate that magnetism partly comes from other fermionic bands which do not cross the Fermi level.<sup>24</sup>

We discuss below several puzzling electronic and magnetic features of the SDW state which have not yet been understood within the itinerant scenario. They include:

(i) A higher conductivity in the SDW state—the system becomes more metallic below  $T_{\text{SDW}}$ . Naively, one would expect a smaller conductivity due to at least partial gapping of the Fermi surfaces (FS). A reduction in the quasiparticle damping, induced by such gapping, may slow down the decrease in conductivity, but the observed increase is highly unlikely for a conventional SDW scenario.

(ii) A significant reconstruction of the electronic dispersion across the SDW transition and complicated FS topology below  $T_{\text{SDW}}$ , with more FS crossings than in the normal state (Refs. 25–28). Some ARPES measurements show<sup>25–27</sup> that in the SDW state visible dispersion remains holelike around the

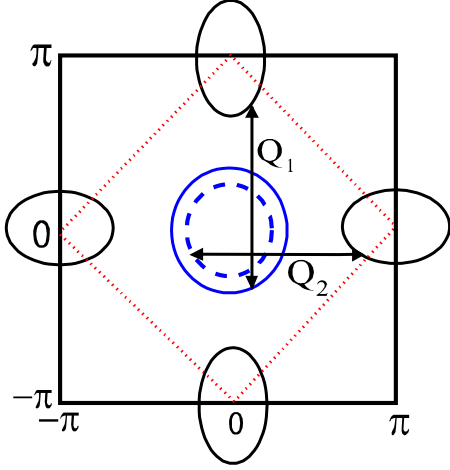


FIG. 1. (Color online) Fermi surface of ferropnictides in the unfolded BZ consisting of two hole pockets centered around the  $\Gamma$  point and two electron pockets centered around  $(\pi, 0)$  and  $(0, \pi)$  points, respectively. The wave vectors  $\mathbf{Q}_1$  and  $\mathbf{Q}_2$  are two degenerate nesting wave vectors.

$\Gamma$  point despite apparent mixing of electron and hole bands while close to  $M=(\pi, \pi)$  point in the folded BZ both electron and hole bands are present. Other measurements<sup>28</sup> indicate that hole and electron pockets are present both near  $M$  and near  $\Gamma$  points.

(iii) The particular  $(0, \pi)$   $(\pi, 0)$  ordering of Fe spins in the unfolded BZ. It is straightforward to obtain  $(\pi, \pi)$  ordering in the folded BZ simply because hole and electron bands are shifted by  $(\pi, \pi)$  in the folded zone. However, SDW order in the folded zone involves two separate magnetic sublattices and unfolding reveals two SDW order parameters (OP)  $\vec{\Delta}_1$  and  $\vec{\Delta}_2$  with momenta  $\mathbf{Q}_1=(0, \pi)$  and  $\mathbf{Q}_2=(\pi, 0)$ , respectively (see Fig. 1). A generic spin configuration then has the form  $\vec{S}(\mathbf{R})=\vec{\Delta}_1 e^{i\mathbf{Q}_1 \cdot \mathbf{R}} + \vec{\Delta}_2 e^{i\mathbf{Q}_2 \cdot \mathbf{R}}$  (the sublattice OPs are  $\vec{\Delta}_1 + \vec{\Delta}_2$  and  $\vec{\Delta}_1 - \vec{\Delta}_2$ ). For such configuration, next-nearest neighbors are antiferromagnetically oriented but the length and the direction of  $\vec{S}$  between nearest neighbors varies. Only if either  $\vec{\Delta}_1$  or  $\vec{\Delta}_2$  vanish, OPs of the two sublattices align parallel or antiparallel to each other, and the spin configuration becomes the same as in the experiments. The issue then is what interaction causes  $\vec{\Delta}_1$  or  $\vec{\Delta}_2$  to vanish.

Another unsolved issues which we do not address here are the absence of magnetism in the nominally undoped LaFePO and LiFeAs compounds and the type of a magnetic order in  $\text{Fe}_{1+x}\text{Te/Se}$  systems. The absence of magnetism in LaFePO and LiFeAs could be due to the fact that these materials are less quasi-two-dimensional, with less nesting.<sup>29</sup> For  $\text{Fe}_{1+x}\text{Te/Se}$ , the experimental data are still controversial.<sup>30</sup>

The full analysis of possible SDW orderings in FeAs systems within a generic four-band model is quite messy and one should have a good starting point to be able to understand the physics. One way to analyze the problem is to solve first the model of four equivalent 2D circular bands (two hole bands and two electron bands) with isotropic interband and intraband interactions, and then introduce anisotropy between the two hole bands, ellipticity of the two electron

bands, and anisotropy of the interactions. This approach has been put forward by Cvetkovic and Tesanovic.<sup>31</sup> They solved exactly the isotropic model and found that SDW state is an insulator—all four Fermi surfaces are fully gapped and that there exists a degenerate manifold of SDW orders. The degeneracy is the same as in  $J_2$  model of localized spins: the SDW order involves two antiferromagnetic sublattices with equal magnitudes of the OPs (i.e.,  $\vec{\Delta}_1 \cdot \vec{\Delta}_2 = 0$ ) but the angle between the two sublattices  $\phi = \cos^{-1}(\Delta_1^2 - \Delta_2^2)/(\Delta_1^2 + \Delta_2^2)$  can be arbitrary. The  $(0, \pi)$  and  $(\pi, 0)$  states belong to this manifold but are not yet selected in the isotropic model. The issue not yet addressed within this approach is what happens with a degenerate manifold once one moves away from the isotropic limit.

Our starting point is different. We use the experimental fact that the two hole FSs are of quite different sizes<sup>26</sup> and assume that one hole band interacts with electron bands much stronger than the other. We then consider, as a first approximation, a three-band model of one hole band centered around  $\Gamma$  point and two electron bands centered around  $(0, \pi)$  and  $(\pi, 0)$ . We solve this model in the mean-field approximation and show that the SDW order is still degenerate for isotropic interactions and circular bands. A degenerate manifold consists of two antiferromagnetic sublattices with generally nonequal magnitudes of the sublattice OPs. The manifold includes  $(0, \pi)$  and  $(\pi, 0)$  states among many others, and the overall symmetry is  $O(6)$ .

In terms of  $\vec{\Delta}_1$  and  $\vec{\Delta}_2$ , the degeneracy implies that the ground-state energy depends only on the combination  $(\vec{\Delta}_1)^2 + (\vec{\Delta}_2)^2$ . The excitation spectrum of such degenerate state contains five Goldstone modes. We then show that the ellipticity of the electron bands and the anisotropy of the interactions breaks the degeneracy and adds to the energy the term  $\beta_{12}|\vec{\Delta}_1|^2|\vec{\Delta}_2|^2$  with positive  $\beta_{12}$ . The full energy is then minimized when either  $\vec{\Delta}_1=0$ , or  $\vec{\Delta}_2=0$ , *ellipticity and the anisotropy of the interactions both select  $(0, \pi)$  or  $(\pi, 0)$  stripe order already at a mean-field level.* This is one of the main results of this paper. A stripe SDW order mixes the hole band and one of the two electron bands but leaves another electron band intact. As a result, the system remains a metal even at strong SDW coupling. We verified that the selection of the stripe order by the interactions between electron states holds only if the interactions are in the charge channel. The same interactions, but in the spin channel, select a different state with  $\vec{\Delta}_1 = \pm \vec{\Delta}_2$ , in which SDW order resides in only one of the two sublattices, see Fig. 2(d).

We did not consider corrections to the mean-field theory (i.e., quantum fluctuations). They are relatively small, at least at weak coupling, although, very likely, they also break  $O(6)$  symmetry. We also do not consider the coupling to the phonons, which is another potential source of symmetry breaking and also pre-emptive tetragonal to orthorhombic transition.<sup>32</sup>

We next consider the role of the second hole band. This band interacts with the electron band left out of the primary SDW mixing. These two bands are less nested and the interaction must exceed a threshold for an additional SDW order to appear. If this is the case and an additional SDW order is strong enough, it gaps the remaining two FSs, and the system

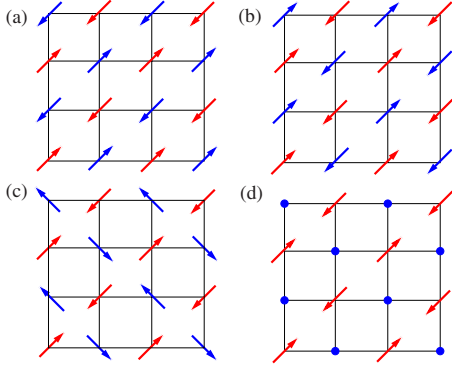


FIG. 2. (Color online) Various SDW spin configurations described by  $\vec{\Delta}_1 e^{iQ_1 R} + \vec{\Delta}_2 e^{iQ_2 R}$ . For the model of Eq. (2), only  $\vec{\Delta}_1^2 + \vec{\Delta}_2^2$  is fixed. Panel (a)  $\vec{\Delta}_1=0$ , panel (b)  $\vec{\Delta}_2=0$ , panel (c)  $\vec{\Delta}_1 \perp \vec{\Delta}_2$ , and panel (d)  $\vec{\Delta}_1 = \vec{\Delta}_2$ .

becomes an insulator. This second (weaker) SDW OP has the momentum  $(0, \pi)$  if the original SDW order was with  $(\pi, 0)$  and vice versa. It then introduces  $\vec{\Delta}_2$  (or  $\vec{\Delta}_1$ ) which was set to zero by the initial selection of  $(0, \pi)$  or  $(\pi, 0)$  order. We show that this second-order parameter is directed orthogonal to the primary one, i.e.,  $\vec{\Delta}_1 \cdot \vec{\Delta}_2 = 0$ . The magnitude of the OP at each Fe site is then the same but the OP is not ferromagnetic along  $x$  or  $y$  direction, i.e., the resulting SDW order is different from  $(0, \pi)$  or  $(\pi, 0)$ . The only way to preserve  $(0, \pi)$  or  $(\pi, 0)$  order in the four-band model is to assume that the interaction between the second hole FS and the electron FS left out in primary SDW selection is below the threshold. Then  $\vec{\Delta}_2$  (or  $\vec{\Delta}_1$ ) remains zero and  $(0, \pi)$  or  $(\pi, 0)$  order survives. A simple but important consequence of this observation is that the four-band model with a stripe order must remain a metal. Specifically, one hole and one electron band are not involved in the SDW mixing and should be observed in ARPES experiments exactly at the same positions as in the normal state: the hole band near  $(0, 0)$  and the electron band near  $(\pi, \pi)$  in the folded BZ. This somewhat unexpected result is another main conclusion of this paper.

Applying the results to the pnictides, where the interactions are believed to be moderate, we show that the hole band with a larger FS interacts more strongly with elliptic electronic bands than the hole band with a smaller FS. Hence, in our theory, the smaller hole FS stays intact below a SDW transition, and the reconstruction of the fermionic structure below  $T_{\text{SDW}}$  involves the larger hole FS and one of two electron FSs. Since the hole FS is a circle and the electron FS are ellipses, the two cross at four points when shifted by, e.g.,  $(0, \pi)$ , and for moderately strong interactions SDW gaps open up only around crossing points.<sup>33</sup> In the folded BZ this gives rise to two FS crossings near either  $(0, 0)$  or  $(\pi, \pi)$ . Adding the FSs which are not involved in the SDW mixing, we find that there generally must be three FS crossings near  $(0, 0)$  or  $(\pi, \pi)$ —more than in the normal state.

Further, our conclusion that  $(0, \pi)$  SDW order in the four-band model preserves metallic behavior even at strong coupling implies that there is no continuous evolution between our four-band model and  $J_1$ - $J_2$  model of localized spins, de-

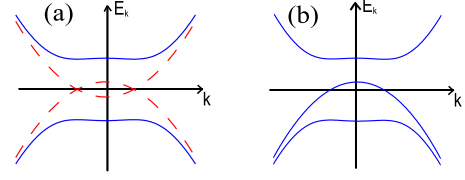


FIG. 3. (Color online) Energy dispersions in the SDW state for full nesting: (a) one-electron band and one hole band and (b) one-electron band and two hole bands. Dashed lines in (a) are the dispersions without SDW order.

spite that quantum fluctuations in  $J_1$ - $J_2$  model select the same  $(0, \pi)$  order. At a first glance, this is surprising as it is well known that in the one-band Hubbard model, there is an evolution from itinerant to localized behavior<sup>34</sup> by which we mean that, upon increasing  $U$ , a one-band system evolves from an antiferromagnetic metal to an antiferromagnetic insulator with the same  $(\pi, \pi)$  magnetic order. To understand why our four-band model is special, we considered a half-filled  $t$ - $t'$ - $U$  Hubbard model on a square lattice with the hopping  $t$  between nearest neighbors and hopping  $t'$  between next-nearest neighbors along the diagonals. In the large  $U$  limit, the model reduces to  $J_1$ - $J_2$  model with  $J_1 \sim t^2/U$  and  $J_2 \sim (t')^2/U$ . As small  $U$ , the model describes two hole bands centered at  $(0, 0)$  and  $(\pi, \pi)$ , and two electron bands centered at  $(\pi, 0)$  and  $(0, \pi)$ . At  $t=0$ , all four bands are identical (up to an overall sign), and all have an isotropic quadratic dispersion near the top of the hole bands and the bottom of the electron bands. For  $t \neq 0$ , electron bands become elliptical near the bottom and the masses of the two hole bands become different (i.e., one hole FS becomes larger and the other becomes smaller). This very much resembles the geometry of our four-band model, except that in  $t$ - $t'$ - $U$  model the second hole band is located at  $(\pi, \pi)$  see Fig. 3. We analyzed  $t$ - $t'$ - $U$  model in the same way as the four-band model and found that in  $t$ - $t'$ - $U$  model there is an evolution from a metallic to an insulating behavior as  $U$  increases. Namely, the state with  $(0, \pi)$  or  $(\pi, 0)$  stripe order is a metal at small  $U$  and an insulator at large  $U$ .

The difference between our case and  $t$ - $t'$ - $U$  model can be easily understood. If we apply the same logics as in our case, i.e., consider the three-band model first, we find  $(0, \pi)$  SDW order which mixes one hole and one electron FSs. The remaining electron band can again mix with the other hole bands and create another SDW order, what eventually gaps all four FSs. However, in  $t$ - $t'$ - $U$  model, the second hole FS is located at  $(\pi, \pi)$  rather than at the  $\Gamma$  point and the second SDW OP has the same momentum  $(0, \pi)$  as the primary SDW OP. As a result, the two OPs just add up and  $(0, \pi)$  order survives. From this perspective, the reason why  $(0, \pi)$  ordered state in the pnictides is a metal is the FS geometry: the fact that both hole FSs are centered at the same  $\Gamma$  point. Were they centered at  $(0, 0)$  and  $(\pi, \pi)$  the system would be a  $(0, \pi)$  metal at weak coupling and  $(0, \pi)$  insulator, described by  $J_1$ - $J_2$  model, at strong coupling.

A word of caution: while it is widely believed, based on band-structure calculations, that both quasi-2D hole FSs in the ferropnictides are centered at  $(0, 0)$  point in both folded and unfolded BZ, experimentally the location of hole pockets



is measured in the folded BZ only. Because  $(\pi, \pi)$  point in the unfolded BZ folds into  $(0,0)$ , the experiments cannot distinguish between the cases when both hole pockets are at  $(0,0)$ , in the unfolded BZ, and when one hole pocket is at  $(0,0)$  and another at  $(\pi, \pi)$ . Still, a good overall agreement between band theory calculations and the data is a strong indicator that the FS geometry predicted by band theory is the correct one. We assume below that this is the case.

In the rest of the paper we discuss these issues in full detail. The structure of the presentation is the following. In Sec. II A we introduce three-band model and discuss SDW ordering in general terms. In Sec. II B we consider the case of circular electron pockets and only the interactions between hole and electron pockets. We show that, at this level, there exists a degenerate manifold of SDW ordered states. In Sec. II C we show that ellipticity of electron pockets and interactions between them remove the degeneracy and select a stripe SDW order already at the mean-field level. In Sec. II C 3 we consider spin component of the interaction between electron pockets and show that it selects a different state in which SDW order appears only at a half of Fe sites.

In Sec. III we add the second hole band and discuss a potential SDW mixing between this band and the electron band left out of SDW mixing in the three-band model. We argue that  $(0, \pi)$  or  $(\pi, 0)$  order survives only if this additional SDW mixing does not happen, i.e., the interaction between these two bands is below the threshold. In Sec. III we contrast this behavior with the one in a  $t$ - $t'$ - $U$  Hubbard model with nearest and next-nearest neighbors. We show that in this model the second hole FS is centered at  $(\pi, \pi)$  (in the unfolded zone) rather than at  $(0,0)$  and the secondary SDW OP has the same momentum as the primary OP, i.e., the stripe order is preserved. We show that  $(0, \pi)$  or  $(\pi, 0)$  state in  $t$ - $t'$ - $U$  model can be either a metal or an insulator, described at strong coupling by  $J_1$ - $J_2$  model. In Sec. IV we consider electronic structure of the SDW phase with  $(0, \pi)$  order and compare our theoretical results with the experiments. We argue that the agreement with ARPES is quite good. We present our conclusions in Sec. V.

Our results are complimentary to earlier arguments as to why SDW phase remains a metal. Ran *et al.*<sup>35</sup> considered an orbital model and argued that the SDW gap must at least have nodes because SDW coupling vanishes along particular directions in  $k$  space. Cvetkovic and Tesanovic<sup>10</sup> and Vorontsov *et al.*<sup>36</sup> argued that a metal survives even for the case of circular FSs, if SDW order is incommensurate. As we said, we argue that the system described by four-band model remains a metal even if the order is commensurate  $(0, \pi)$  or  $(\pi, 0)$  and the interactions are angle independent. Our analysis also serves as a justification to the works<sup>37,38</sup> which discussed the consequences of the  $(\pi, 0)$  SDW order in itinerant models without analyzing why this order is selected. Some of our results are also consistent with the analysis of possible magnetically ordered states in the two-orbital model by Lorenzana *et al.*<sup>39</sup> We also found, for a particular model, a state with magnetic order residing only on one of the two sublattices. Such state was identified as a possible candidate in a generic Landau-theory analysis for a two-sublattice order parameter.<sup>39</sup>

## II. ITINERANT SDW ORDER IN THE THREE-BAND MODEL

### A. General consideration

Consider a model of interacting fermions with a circular hole FS centered around  $\Gamma$  point ( $\alpha$  band) and two elliptical electron Fermi-surface pockets centered around  $(\pm \pi, 0)$  and  $(0, \pm \pi)$  points in the unfolded BZ ( $\beta$  bands) (see Fig. 1)

$$H_2 = \sum_{\mathbf{p}, \sigma} [\varepsilon_{\mathbf{p}}^{\alpha} \alpha_{\mathbf{p}\sigma}^{\dagger} \alpha_{\mathbf{p}\sigma} + \varepsilon_{\mathbf{p}}^{\beta_1} \beta_{\mathbf{p}\sigma}^{\dagger} \beta_{\mathbf{p}\sigma} + \varepsilon_{\mathbf{p}}^{\beta_2} \beta_{\mathbf{p}\sigma}^{\dagger} \beta_{\mathbf{p}\sigma}]. \quad (1)$$

Here  $\varepsilon_{\mathbf{p}}^{\alpha} = -\frac{\hbar^2 p^2}{2m_1} + \mu$ ,  $\varepsilon_{\mathbf{p}}^{\beta_1} = \frac{\hbar^2 p_x^2}{2m_x} + \frac{\hbar^2 p_y^2}{2m_y} - \mu$ , and  $\varepsilon_{\mathbf{p}}^{\beta_2} = \frac{\hbar^2 p_x^2}{2m_y} + \frac{\hbar^2 p_y^2}{2m_x} - \mu$  are the dispersions of hole and electron bands. The momenta of  $\alpha$  fermions are counted from  $(0,0)$ , the momenta of  $\beta_1$  and  $\beta_2$  fermions are counted from  $(0, \pi)$  and  $(\pi, 0)$ , respectively.

The interacting part of the Hamiltonian contains density-density interactions involving  $\alpha$  and  $\beta$  fermions (interactions with small momentum transfer),  $(\pi, 0)$ ,  $(0, \pi)$ , and  $(\pi, \pi)$  scattering processes, and umklapp pair hopping terms.<sup>12</sup> Consider first only the interactions between hole and electron bands, which give rise to a SDW order. These are density-density interaction between  $\alpha$  and  $\beta$  fermions, and the pair hopping term<sup>12</sup>

$$H_4 = U_1 \sum \alpha_{\mathbf{p}_3\sigma}^{\dagger} \beta_{\mathbf{p}_4\sigma'}^{\dagger} \beta_{\mathbf{p}_2\sigma'} \alpha_{\mathbf{p}_1\sigma} + \frac{U_3}{2} \sum [\beta_{\mathbf{p}_3\sigma}^{\dagger} \beta_{\mathbf{p}_4\sigma'}^{\dagger} \alpha_{\mathbf{p}_2\sigma'} \alpha_{\mathbf{p}_1\sigma} + \text{H.c.}]. \quad (2)$$

We neglect potential angular dependencies of  $U_1$  and  $U_3$  along the FSs.

Because  $U_1$  and  $U_3$  involve  $\beta_1$  and  $\beta_2$  fermions, we have to introduce two SDW OPs  $\vec{\Delta}_1 \propto \sum_{\mathbf{p}} \langle \alpha_{\mathbf{p}\delta}^{\dagger} \beta_{\mathbf{p}\gamma} \vec{\sigma}_{\delta\gamma} \rangle$  with momentum  $\mathbf{Q}_1 = (0, \pi)$  and  $\vec{\Delta}_2 \propto \sum_{\mathbf{p}} \langle \alpha_{\mathbf{p}\delta}^{\dagger} \beta_{\mathbf{p}\gamma} \vec{\sigma}_{\delta\gamma} \rangle$  with momentum  $\mathbf{Q}_2 = (\pi, 0)$ . Without loss of generality we can set  $\vec{\Delta}_1$  along  $z$  axis and  $\vec{\Delta}_2$  in the  $xz$  plane. In explicit form, we introduce

$$\begin{aligned} \Delta_1^z &= -U_{\text{SDW}} \sum_{\mathbf{p}} \langle \alpha_{\mathbf{p}\uparrow}^{\dagger} \beta_{\mathbf{p}\uparrow} \rangle, \\ \Delta_2^{z(x)} &= -U_{\text{SDW}} \sum_{\mathbf{p}} \langle \alpha_{\mathbf{p}\uparrow}^{\dagger} \beta_{\mathbf{p}\uparrow(\downarrow)} \rangle, \end{aligned} \quad (3)$$

where  $U_{\text{SDW}} = U_1 + U_3$ .

### B. Degeneracy of the SDW order

Assume first that electron pockets are circular, i.e.,  $m_x = m_y$  and  $\varepsilon_{\mathbf{p}}^{\beta_1} = \varepsilon_{\mathbf{p}}^{\beta_2} = \varepsilon_{\mathbf{p}}^{\beta}$ , i.e.,  $m_1 = m_x = m_y$ . In this situation, the Hamiltonian, Eq. (2), can be easily diagonalized by performing three subsequent Bogolyubov transformations. First

$$\begin{aligned} \beta_{2\mathbf{p}\uparrow} &= \beta_{2\mathbf{p}a} \cos \eta - \beta_{2\mathbf{p}b} \sin \eta, \\ \beta_{2\mathbf{p}\downarrow} &= \beta_{2\mathbf{p}a} \sin \eta + \beta_{2\mathbf{p}b} \cos \eta \end{aligned} \quad (4)$$

with  $\cos \eta = \frac{\Delta_1^z}{\Delta_2}$ ,  $\sin \eta = \frac{\Delta_2^x}{\Delta_2}$ , and  $\Delta_2 = \sqrt{(\Delta_2^x)^2 + (\Delta_2^z)^2}$ . This transformation rotates the quantization axis of  $\vec{\Delta}_2$  and makes it parallel to  $\vec{\Delta}_1$ . Then

$$\begin{aligned}
\beta_{1p\uparrow} &= c_{ap} \cos \theta - d_{ap} \sin \theta, \\
\beta_{2pa} &= c_{ap} \sin \theta + d_{ap} \cos \theta, \\
\beta_{1p\downarrow} &= c_{bp} \cos \theta - d_{bp} \sin \theta, \\
\beta_{2pb} &= c_{bp} \sin \theta + d_{bp} \cos \theta
\end{aligned} \tag{5}$$

with  $\cos \theta = \frac{\tilde{\Delta}_1}{\Delta}$ ,  $\sin \theta = \frac{\tilde{\Delta}_2}{\Delta}$ , and  $\Delta = \sqrt{(\tilde{\Delta}_1)^2 + (\tilde{\Delta}_2)^2}$ . This mixes order parameters  $\tilde{\Delta}_1$  and  $\tilde{\Delta}_2$  into one, combined order parameter  $\Delta$ . Once we are left with only one order parameter, bilinear in fermions, we can diagonalize the quadratic form by a usual Bogolyubov rotation

$$\begin{aligned}
\alpha_{1p\uparrow} &= p_{ap} \cos \psi + e_{ap} \sin \psi, \\
\alpha_{1p\downarrow} &= p_{bp} \cos \tilde{\psi} + e_{bp} \sin \tilde{\psi}
\end{aligned} \tag{6}$$

and

$$\begin{aligned}
c_{ap} &= e_{ap} \cos \psi - p_{ap} \sin \psi, \\
c_{bp} &= e_{bp} \cos \tilde{\psi} - p_{bp} \sin \tilde{\psi},
\end{aligned} \tag{7}$$

where  $\tilde{\psi} = \frac{\pi}{2} + \psi$ ,  $\cos^2 \psi$ ,  $\sin^2 \psi = \frac{1}{2} [1 \pm \frac{e_p}{\sqrt{(\varepsilon_p)^2 + \Delta^2}}]$ , and  $\varepsilon_p = \frac{1}{2} [\varepsilon_p^{\alpha 1} - \varepsilon_p^{\beta}]$ . The resulting quadratic Hamiltonian becomes

$$\begin{aligned}
H_2^{eff} &= \sum_{a,p} \varepsilon_p^\beta d_{ap}^\dagger d_{ap} + \sum_p E_p (e_{ap}^\dagger e_{ap} + p_{bp}^\dagger p_{bp} \\
&\quad - e_{bp}^\dagger e_{bp} - p_{ap}^\dagger p_{ap}),
\end{aligned} \tag{8}$$

where  $E_p = \pm \sqrt{(\varepsilon_p)^2 + |\Delta|^2}$ . The self-consistent equation for the gap reduces to

$$1 = \frac{U_{SDW}}{2N} \sum_p \frac{1}{\sqrt{(\varepsilon_p)^2 + \Delta^2}}. \tag{9}$$

Two key observations follow from these results. First, self-consistency equation Eq. (9) sets the value of the total order parameter  $\tilde{\Delta}_1^2 + \tilde{\Delta}_2^2$  but does not specify what  $\tilde{\Delta}_1$  and  $\tilde{\Delta}_2$  are. The implication is that, at this level, the OP manifold can be viewed as a six-component vector (three components of  $\tilde{\Delta}_1$  and three of  $\tilde{\Delta}_2$ ), SDW ordering is a spontaneous breaking of  $O(6)$  symmetry, and an ordered state has five Goldstone modes. The degenerate ground-state manifold is composed of two-sublattice states with antiferromagnetic order along diagonals;  $(0, \pi)$  or  $(\pi, 0)$  states, for which  $\tilde{\Delta}_1 = 0$  or  $\tilde{\Delta}_2 = 0$ , are just two of many possibilities (see Fig. 2). Second, a linear combination of original electronic operators described by  $d_{a,p}$  decouples from the SDW procedure. Then, even in case of perfect nesting, when  $\varepsilon_p^{\alpha 1} = -\varepsilon_p^{\beta}$ , the system still remains a metal in the SDW phase—excitations described by  $e_{a,p}$  and  $p_{a,p}$  operators become gapped but excitations described by  $d_{a,p}$  operators remain gapless.

Note that the ground-state degeneracy is even larger than in the  $J_1$ - $J_2$  model of localized spins—not only the angle between the two sublattices can be arbitrary but also the magnitudes of the ordered moments in the two sublattices can be different. To confirm this result, we computed the

ground-state energy  $E_{gr}$  in the mean-field approximation and indeed found that it depends only on  $\tilde{\Delta}_1^2 + \tilde{\Delta}_2^2$ . We also extended this analysis to include  $\alpha$ - $\beta$  interactions with momentum transfer  $(0, \pi)$  and  $(\pi, 0)$  ( $U_2$  terms in the terminology of Ref. 12) and still found the same degeneracy.

Note by passing that the momentum integration in the self-consistency condition, Eq. (9) is *not* restricted to the FS, and a finite SDW order parameter  $\Delta$  appears even when FS disappear. This is due to the fact that a particle-hole bubble made out of  $\alpha$  and  $\beta$  fermions actually behaves as a particle-particle bubble because of sign difference in fermionic dispersions of  $\alpha$  and  $\beta$  fermions. The consequence is that the SDW ordered moment does not scale with the (small) sizes of the hole and electrons FSs. In other words, SDW order is due to dispersion nesting of  $\alpha$  and  $\beta$  fermions but *not due to FS nesting*.

## C. Selection of the SDW order

### 1. Interaction between electron pockets

We now add the interactions between the two electron pockets and verify whether they lift the degeneracy. These interaction do not contribute to the quadratic form but they do contribute to the  $\Delta$  dependence of the ground-state energy. It has been argued,<sup>3</sup> based on the transformation of the underlying orbital model into a band model, that the interactions between the two electron pockets are not particularly small and must be included into the theory.

There are four possible  $\beta$ - $\beta$  interactions:

$$\begin{aligned}
H_4^{ex} &= U_6 \sum \beta_{1p_3\sigma}^\dagger \beta_{2p_4\sigma'}^\dagger \beta_{2p_2\sigma'} \beta_{1p_1\sigma} \\
&\quad + U_7 \sum \beta_{2p_3\sigma}^\dagger \beta_{1p_4\sigma'}^\dagger \beta_{2p_2\sigma'} \beta_{1p_1\sigma} \\
&\quad + \frac{U_8}{2} \sum [\beta_{2p_3\sigma}^\dagger \beta_{2p_4\sigma'}^\dagger \beta_{1p_2\sigma'} \beta_{1p_1\sigma} + \text{H.c.}] \\
&\quad + \frac{U_4}{2} \sum \left[ \sum \beta_{1p_3\sigma}^\dagger \beta_{1p_4\sigma'}^\dagger \beta_{1p_2\sigma'} \beta_{1p_1\sigma} \right. \\
&\quad \left. + \beta_{2p_3\sigma}^\dagger \beta_{2p_4\sigma'}^\dagger \beta_{2p_2\sigma'} \beta_{2p_1\sigma} \right].
\end{aligned} \tag{10}$$

(we used the terminology consistent with Ref. 12). It is natural to assume that all interactions are repulsive, i.e., all  $U_i > 0$ .

Applying the sequence of Bogolyubov transformations and taking  $\langle \dots \rangle$ , we obtain the contribution to the ground-state energy from various terms in Eq. (10)

$$\begin{aligned}
U_6 \sum \beta_{1p_3\sigma}^\dagger \beta_{2p_4\sigma'}^\dagger \beta_{2p_2\sigma'} \beta_{1p_1\sigma} &\rightarrow 2A^2 \frac{|\tilde{\Delta}_1|^2 |\tilde{\Delta}_2|^2}{\Delta^4} + \dots, \\
U_7 \sum \beta_{2p_3\sigma}^\dagger \beta_{1p_4\sigma'}^\dagger \beta_{2p_2\sigma'} \beta_{1p_1\sigma} &\rightarrow 2A^2 \left( 2 \frac{(\tilde{\Delta}_1 \cdot \tilde{\Delta}_2)^2}{\Delta^4} - \frac{|\tilde{\Delta}_1|^2 |\tilde{\Delta}_2|^2}{\Delta^4} \right) + \dots, \\
U_8 \sum [\beta_{2p_3\sigma}^\dagger \beta_{2p_4\sigma'}^\dagger \beta_{1p_2\sigma'} \beta_{1p_1\sigma} + \text{H.c.}] &\rightarrow 4A^2 \frac{|\tilde{\Delta}_1|^2 |\tilde{\Delta}_2|^2}{\Delta^4},
\end{aligned}$$

$$U_4 \sum [\sum \beta_{1\mathbf{p}_3\sigma}^\dagger \beta_{1\mathbf{p}_4\sigma'}^\dagger \beta_{1\mathbf{p}_2\sigma'} \beta_{1\mathbf{p}_1\sigma} + \beta_{2\mathbf{p}_3\sigma}^\dagger \beta_{2\mathbf{p}_4\sigma'}^\dagger \beta_{2\mathbf{p}_2\sigma'} \beta_{2\mathbf{p}_1\sigma}] \rightarrow -4A^2 \frac{|\vec{\Delta}_1|^2 |\vec{\Delta}_2|^2}{\Delta^4}, \quad (11)$$

where dots stand for the terms which depend only on  $\Delta^2$  and do not break a degeneracy, and  $A = (c - d)$ , where  $c = \langle c_{b\mathbf{p}}^\dagger c_{b\mathbf{p}} \rangle = \langle c_{a\mathbf{p}}^\dagger c_{a\mathbf{p}} \rangle = \frac{1}{2N} \sum_{\mathbf{p}} (1 - \frac{\varepsilon_{\mathbf{p}}}{\sqrt{(\varepsilon_{\mathbf{p}})^2 + \Delta^2}})$  and  $d = \langle d_{b\mathbf{p}}^\dagger d_{b\mathbf{p}} \rangle = \langle d_{a\mathbf{p}}^\dagger d_{a\mathbf{p}} \rangle = \frac{1}{2N} \sum_{\mathbf{p}} (1 - \frac{E_{\mathbf{p}}}{|E_{\mathbf{p}}|})$ . The quantity  $A$  is zero in the normal state but has a finite value in the SDW state. Combining all contributions, we obtain

$$E_{gr}^{ex} = 2A^2 [(U_6 + U_8 - U_7 - U_4)] \frac{|\vec{\Delta}_1|^2 |\vec{\Delta}_2|^2}{\Delta^4} + 4A^2 U_7 \frac{(\vec{\Delta}_1 \cdot \vec{\Delta}_2)^2}{\Delta^4}. \quad (12)$$

We see that  $E_{gr}^{ex}$  depends on  $|\vec{\Delta}_1|^2 |\vec{\Delta}_2|^2$  and on  $(\vec{\Delta}_1 \cdot \vec{\Delta}_2)^2$ , i.e., it is sensitive to both, relative values and relative directions of  $\vec{\Delta}_1$  and  $\vec{\Delta}_2$ . When all interactions are of equal strength, the first term vanishes, and the last term favors  $\vec{\Delta}_1 \perp \vec{\Delta}_2$ . In this situation, the  $O(6)$  degeneracy is broken, but only down to  $O(3) \times O(2)$ , i.e., the magnitude of the order parameter at each site is now the same because  $(\vec{\Delta}_1 + \vec{\Delta}_2)^2 = (\vec{\Delta}_1 - \vec{\Delta}_2)^2$ , but the angle between the directions of the SDW order in the two sublattices (i.e., between  $\vec{\Delta}_1 + \vec{\Delta}_2$  and  $\vec{\Delta}_1 - \vec{\Delta}_2$ ) is still arbitrary. This is exactly the same situation as in the classical  $J_1$ - $J_2$  model. However, once  $U_6 + U_8 - U_7 - U_4$  is nonzero, the degeneracy is broken down to a conventional  $O(3)$  already at the mean-field level. Because  $U_4$  is reduced and even changes sign under the renormalization group (RG),<sup>12</sup> while other  $U_i$  do not flow, the most likely situation is that  $U_6 + U_8 - U_7 - U_4 > 0$ , in which case  $E_{gr}^{ex}$  is minimized when either  $\vec{\Delta}_1 = 0$ , or  $\vec{\Delta}_2 = 0$ , i.e., SDW order is either  $(0, \pi)$  or  $(\pi, 0)$ . This is exactly the same SDW order as observed in the experiments. If  $U_6 + U_8 - U_7 - U_4$  was negative,  $E_{gr}^{ex}$  would be minimized when  $|\vec{\Delta}_1| = |\vec{\Delta}_2|$ , in which case the SDW OPs of the two sublattices would align orthogonal to each other. The spin configuration for such state is shown in Fig. 2(c). Such orthogonal spin configuration has been found in the analysis of spin ordering in the two-orbital model.<sup>39</sup>

## 2. Deviations from perfect nesting

Consider next what happens when we also include into consideration the fact that electronic pockets are actually ellipses rather than circles, i.e., the effective masses  $m_x$  and  $m_y$  are not equal, and  $\varepsilon_{\mathbf{k}}^{\beta_1} \neq \varepsilon_{\mathbf{k}}^{\beta_2}$ . To continue with the analytical analysis, we assume that the ellipticity is small, introduce  $m_x = (1 + \delta)m$  and  $m_y = (1 - \delta)m$ , where  $\delta \ll 1$ , and compute the correction to the ground-state energy to second order in  $\delta$ . Performing the same set of transformations as before, we find that, for a nonzero  $\delta$ , Eq. (8) has to be supplemented by

$$H_4^{(1)} = 2\delta \sum_{\mathbf{p}} \frac{p_x^2 - p_y^2}{2m} \{ \cos 2\theta [\cos^2 \psi \rho_{a\mathbf{p}}^\dagger e_{a\mathbf{p}} + \sin^2 \psi p_{a\mathbf{p}}^\dagger p_{a\mathbf{p}} - d_{a\mathbf{p}}^\dagger d_{a\mathbf{p}} - \sin \psi \cos \psi (p_{a\mathbf{p}}^\dagger e_{a\mathbf{p}} + \text{H.c.})] + \sin 2\theta [\cos \psi (p_{a\mathbf{p}}^\dagger d_{a\mathbf{p}} + \text{H.c.}) - \sin \psi (p_{e\mathbf{p}}^\dagger d_{a\mathbf{p}} + \text{H.c.})] \}, \quad (13)$$

where the angles  $\theta$  and  $\psi$  are defined in the same way as before, and the overall factor of 2 accounts for spin degeneracy. For a perfect nesting  $e_a[p_a]$  states are all empty (occupied) and for small  $\delta \ll \Delta$  ellipticity does not change this.

From Eq. (13) we obtain two contributions to  $E_{gr}$  of order  $\delta^2$ . One comes from virtual transitions to nonoccupied states and is negative. Another comes from the change in the dispersion of the ungapped  $\varepsilon_{\mathbf{k}}^{\beta_1}$  in the presence of ellipticity and is positive. The negative contribution comes from nondiagonal terms in Eq. (13) taken to second order. Applying a standard second-order quantum-mechanical perturbation theory we obtain

$$E_{gr}^{a,ellipt} = -\delta^2 \sin^2 2\theta \times \sum_{\mathbf{p}} \left( \frac{p_x^2 - p_y^2}{2m} \right)^2 \frac{\Delta^2}{2E_{\mathbf{p}}} \left[ \frac{1}{(E_{\mathbf{p}} + |\varepsilon_{\mathbf{p}}|)^2} - \frac{1}{(2E_{\mathbf{p}})^2} \right] + \dots, \quad (14)$$

where  $\varepsilon_{\mathbf{p}}$  and  $E_{\mathbf{p}}$  are defined after Eq. (8), and dots stand for the terms which do not depend on  $\theta$  and do not break the degeneracy. We remind that  $\cos \theta = |\vec{\Delta}_1|/\Delta$  and  $\sin \theta = |\vec{\Delta}_2|/\Delta$  so that  $\sin^2(2\theta) = 4|\vec{\Delta}_1|^2 |\vec{\Delta}_2|^2 / \Delta^4$ . Replacing the sum in Eq. (14) by the integral and rescaling, we obtain for the energy per unit area

$$E_{gr}^{a,ellipt} = -\delta^2 \sin^2 2\theta \frac{m\nu^2}{16\pi} F\left(\frac{\mu}{\Delta}\right), \quad (15)$$

where

$$F(x) = \frac{2}{x^2} \int_{-x}^{\infty} \frac{(y+x)^2 dy}{\sqrt{y^2+1}} \left[ \frac{1}{(\sqrt{y^2+1} + |y|)^2} - \frac{1}{4(y^2+1)} \right]. \quad (16)$$

At large  $x$ , i.e., at small  $\Delta/\mu$ , expected within the itinerant description,  $F(x \rightarrow \infty) \approx 1$ , and  $E_{gr}^{a,ellipt}$  becomes

$$E_{gr}^{a,ellipt} = -\delta^2 \sin^2 2\theta \frac{m\mu^2}{16\pi}. \quad (17)$$

Another contribution to  $E_{gr}$  comes from the diagonal term in Eq. (13) and is related to  $\delta$ -induced change in the dispersion of  $d$  fermions, which are not gapped by SDW. Adding  $-\delta(p_x^2 - p_y^2)/m$  term from Eq. (13) to the dispersion of a  $d$  fermion and evaluating the energy of the occupied states, we obtain after simple algebra that a linear term in  $\delta$  is canceled out but  $\delta^2$  term is finite and yields

$$E_{gr}^{b,ellipt} = +\delta^2 \sin^2 2\theta \frac{m\mu^2}{8\pi}. \quad (18)$$

Comparing the two contributions, we find that  $E_{gr}^{b,ellipt}$  is two times larger than  $E_{gr}^{a,ellipt}$ . Adding the two terms and expressing  $\sin^2 2\theta$  in terms of  $\Delta_1$  and  $\Delta_2$ , we obtain

$$E_{gr}^{ellipt} = C |\vec{\Delta}_1|^2 |\vec{\Delta}_2|^2, \quad C = \delta^2 \frac{m\mu^2}{4\pi\Delta^4}. \quad (19)$$

We see that  $C$  is positive, i.e., the correction due to ellipticity of electron pockets breaks the degeneracy and selects either  $(0, \pi)$  or  $(\pi, 0)$  state. This is again the same selection as one

needs for consistency with the experiments. We found it quite remarkable that ellipticity introduces effective interaction between two SDW OPs which, for  $\Delta \ll \mu$ , leads to the same selection of the ground-state SDW order as the direct interaction between the two electron pockets.

For larger  $\Delta/\mu$ ,  $F(x)$  increases, eventually to  $F(x \ll 1) = (1/2)(0.25/x)^2$ , and  $E_{gr}^{a,ellipt}$  becomes larger than  $E_{gr}^{b,ellipt}$ . The sign change in  $E_{gr}^{ellipt}$  occurs, however, at quite large  $\Delta \geq \mu/2$  which very likely is not realized in the ferropnictides.

The issue we did not address in this work is how the angular dependence of the interaction contributes to the selection of the SDW order. The angular dependence of intrapocket and inter-pocket interactions originates from the fact that fermionic states at different parts of hole and electron FSs represent different orbital configurations in the underlying orbital model. Once one moves from orbital to band representation, fermionic excitations become isotropic along the FS, and the information about the orbital structure is passed to interactions in the form of angular dependence. The angular dependence of the interaction was argued to be essential for the understanding of an extended  $s$ -wave superconductivity with nodes along the electron FSs (Ref. 3) but to what extent it is relevant to magnetism is not yet known.

### 3. Selection of the SDW order in the itinerant $J_1$ - $J_2$ model

We next show that the selection of the  $(0, \pi)$  and  $(\pi, 0)$  states in the itinerant model occurs only if fermion-fermion interactions are conventional charge-charge interactions rather than spin-spin interactions (the vertices contain spin  $\delta$  functions rather than  $\sigma$  matrices). Briefly, we consider the itinerant  $J_1$ - $J_2$  model with spin-spin interaction and show that this model also possesses  $O(6)$  symmetry at the mean-field level but the magnetic order selected by quartic terms is different from  $(0, \pi)$ .

The itinerant  $J_1$ - $J_2$  model is described by

$$H^{J_1-J_2} = \sum \tilde{S}(\mathbf{p}) \tilde{S}(-\mathbf{p}) \times [J_1(\cos p_x + \cos p_y) + 2J_2 \cos p_x \cos p_y], \quad (20)$$

where  $\tilde{S}(\mathbf{p}) = (1/2) \sum_{\mathbf{p}_1} a_{\mathbf{p}_1}^\dagger \tilde{\sigma}_{\alpha\beta} a_{\mathbf{p}_1+\mathbf{p}}^\dagger$ , where  $a$  are fermionic operators which can be either holes, when  $\mathbf{p}_1$  is close to  $(0,0)$ , or electrons, when  $\mathbf{p}_1$  is close to  $(0, \pi)$  or  $(\pi, 0)$ . The kinetic-energy term is the same as in Eq. (1). To avoid misunderstanding, we emphasize that the itinerant  $J_1$ - $J_2$  model considered here is not the model of localized spins, even when  $J_{1,2}$  is large compared to the Fermi energy. In particular, there is no constraint of no-double occupancy, like the one in  $t$ - $J$  model for the cuprates. We consider the localized  $J_1$ - $J_2$  model later in the paper.

Relevant momenta  $\mathbf{p}$  in Eq. (20) are near  $(0,0)$ ,  $(0, \pi)$ ,  $(\pi, 0)$ , and  $(\pi, \pi)$ . Equation (2) is reproduced if we consider the contributions with  $\mathbf{p}$  near  $(0,0)$ ,  $(0, \pi)$ , and  $(\pi, 0)$ . One can easily verify that each of these terms has contributions which mix  $\alpha$  and  $\beta$  operators. Expressing  $\mathbf{S}$  in terms of bilinear combinations of fermions and using the spin algebra we obtain that for itinerant  $J_1$ - $J_2$  model  $U_3 = 3J_2$  and  $U_1 = J_2 - J_1$ , such that, for this model,  $U_{SDW} = U_1 + U_3 = J_{SDW} = 4J_2 - J_1$ . We then introduce the same SDW vector OPs

as in Eq. (3):  $\Delta_1^z = -J_{SDW} \sum_{\mathbf{p}} \langle \alpha_{1\mathbf{p}}^\dagger \beta_{1\mathbf{p}} \rangle$  and  $\Delta_2^{z(x)} = -J_{SDW} \sum_{\mathbf{p}} \langle \alpha_{1\mathbf{p}}^\dagger \beta_{2\mathbf{p}(\perp)} \rangle$ . Performing the same mean-field decoupling of the four-fermion terms as in the previous section, we find that self-consistency equations for  $\tilde{\Delta}_1$  and  $\tilde{\Delta}_2$  are again identical and only specify the value of  $\Delta^2 = |\tilde{\Delta}_1|^2 + |\tilde{\Delta}_2|^2$

$$1 = \frac{J_{SDW}}{2N} \sum_{\mathbf{p}} \frac{1}{\sqrt{(\epsilon_{\mathbf{p}})^2 + \Delta^2}}. \quad (21)$$

The solution for  $\Delta$  exists for  $J_2 > J_1/4$ , i.e., for large  $J_2$  SDW order is antiferromagnetic along the diagonals. The condition  $J_2 > J_1/4$  is similar to  $J_2 > J_1/2$  for a classical  $J_1$ - $J_2$  model of localized spins (the conditions in itinerant and localized models do not have to be exactly the same, indeed).

The degeneracy between different SDW states with the same  $\Delta^2$  is again broken once we include interactions between electron pockets. Such interactions are generated by  $J_1$  and  $J_2$  terms taken at momenta  $\mathbf{p} = (0,0)$  and  $(\pi, \pi)$ . One can easily verify that these the  $(\pi, \pi)$  term mixes the two electronic operators and contribute terms equivalent to  $U_6$ ,  $U_7$ , and  $U_8$  terms in Eq. (10) while from  $(0,0)$  term one obtains contributions equivalent to  $U_6$  and  $U_4$  terms in Eq. (10).

Re-expressing  $\tilde{S}(\mathbf{p}) \tilde{S}(-\mathbf{p})$  in terms of fermions we obtain the quartic interaction between  $\beta_1$  and  $\beta_2$  fermions in the same form as in Eq. (11) with the coefficients

$$U_6^s = J_1 - 3J_2, \quad U_7^s = -J_1 - 3J_2, \\ U_8^s = 3(J_1 - J_2), \quad U_4^s = -3(J_1 + J_2). \quad (22)$$

Substituting these coefficients into Eq. (12), we obtain

$$E_{gr}^{J_1-J_2} = 4A^2 \left[ 4J_1 \frac{|\tilde{\Delta}_1|^2 |\tilde{\Delta}_2|^2}{\Delta^4} - (J_1 + 3J_2) \frac{(\tilde{\Delta}_1 \cdot \tilde{\Delta}_2)^2}{\Delta^4} \right], \quad (23)$$

where  $A > 0$  is defined after Eq. (12). Comparing this form with Eq. (12) we see that now the prefactor for  $(\tilde{\Delta}_1 \cdot \tilde{\Delta}_2)^2$  term is negative, i.e., the energy is lowered when  $\tilde{\Delta}_1$  and  $\tilde{\Delta}_2$  are parallel. The terms  $|\tilde{\Delta}_1|^2 |\tilde{\Delta}_2|^2$  and  $(\tilde{\Delta}_1 \cdot \tilde{\Delta}_2)^2$  are then equal, and from Eq. (23) we obtain

$$E_{gr}^{J_1-J_2} = -12A^2 (J_2 - J_1) \frac{|\tilde{\Delta}_1|^2 |\tilde{\Delta}_2|^2}{\Delta^4}. \quad (24)$$

We see that the state with  $\tilde{\Delta}_1 = 0$  or  $\tilde{\Delta}_2 = 0$ , which has  $(0, \pi)$  or  $(\pi, 0)$  order, is only favored in the range  $J_1/4 < J_2 < J_1$ . For larger  $J_2$ , the energy is minimized when  $\tilde{\Delta}_1 = \pm \tilde{\Delta}_2$ . The corresponding SDW state has antiferromagnetic order for spins in one sublattice but no SDW order for spins in the other sublattice [see Fig. 2(d)]. Such state has been identified as one of possible candidates for the magnetic ground state in the generic analysis of the Landau theory for a two-component order parameter.<sup>39</sup> We see therefore that, when  $J_2$  term dominates, spin-spin interaction between the two electron bands selects different SDW order from the case when the interaction is in the charge channel.



### III. SDW ORDER IN FOUR-BAND MODEL

So far we found that the stripe  $(\pi, 0)$  or  $(0, \pi)$  order is selected in the three-band model (one hole and two electron FSs) with conventional charge interactions. We now add the second hole pocket and check how its inclusion affects the SDW order.

As we said in the Introduction, the second hole FS is less coupled to electron FSs than the one that we already included into the three-band model. This is due to a combination of the two factors: the difference in the interactions  $U_{\text{SDW}}$  and the difference in the degree of the overlap with the elliptic electron FSs. We consider both factors.

To begin, consider a model of two circular hole FSs and two circular electron FSs. Let's assume that all FSs are of the same size but that there are two different SDW interactions between hole and electron bands— $U_{\text{SDW}}^{(1)}$  for one hole band and  $U_{\text{SDW}}^{(2)}$  for the other. We introduce four SDW OPs:  $\tilde{\Delta}_{11}$ ,  $\tilde{\Delta}_{12}$ ,  $\tilde{\Delta}_{21}$ , and  $\tilde{\Delta}_{22}$ , of which  $\tilde{\Delta}_{11}$  and  $\tilde{\Delta}_{21}$  are with momentum  $\mathbf{Q}_1$ , and  $\tilde{\Delta}_{12}$  and  $\tilde{\Delta}_{22}$  are with momentum  $\mathbf{Q}_2$ . The OPs  $\tilde{\Delta}_{11}$  and  $\tilde{\Delta}_{12}$  involve fermions from the first hole band while  $\tilde{\Delta}_{21}$ , and  $\tilde{\Delta}_{22}$  involve fermions from the second hole band. Without loss of generality,  $\tilde{\Delta}_{11}$  can be directed along  $z$  axis, and  $\tilde{\Delta}_{12}$  in the  $xz$  plane, but the directions of  $\tilde{\Delta}_{21}$  and  $\tilde{\Delta}_{22}$  can be arbitrary in 3D space. To simplify the discussion, we assume that the SDW configuration is coplanar, and set  $\tilde{\Delta}_{11}$  and  $\tilde{\Delta}_{21}$  to be along  $z$  axis, and  $\tilde{\Delta}_{12}$  and  $\tilde{\Delta}_{22}$  to be along  $x$  axis. In explicit form, we then have, by analogy with Eq. (3)

$$\begin{aligned}\tilde{\Delta}_{11} &= \Delta_1^z = -U_{\text{SDW}}^{(1)} \sum_{\mathbf{p}} \langle \alpha_{1\mathbf{p}\uparrow}^\dagger \beta_{1\mathbf{p}\uparrow} \rangle, \\ \tilde{\Delta}_{12} &= \Delta_1^x = -U_{\text{SDW}}^{(1)} \sum_{\mathbf{p}} \langle \alpha_{1\mathbf{p}\uparrow}^\dagger \beta_{2\mathbf{p}\downarrow} \rangle, \\ \tilde{\Delta}_{21} &= \Delta_2^z = -U_{\text{SDW}}^{(2)} \sum_{\mathbf{p}} \langle \alpha_{2\mathbf{p}\uparrow}^\dagger \beta_{1\mathbf{p}\uparrow} \rangle, \\ \tilde{\Delta}_{22} &= \Delta_2^x = -U_{\text{SDW}}^{(2)} \sum_{\mathbf{p}} \langle \alpha_{2\mathbf{p}\uparrow}^\dagger \beta_{2\mathbf{p}\downarrow} \rangle.\end{aligned}\quad (25)$$

From now on the subindices 1 and 2 indicate SDW OPs associated with one or the other hole bands.

As in previous section, we first consider only the interactions between hole and electron states which contribute to the SDW order ( $U_1$  and  $U_3$  terms). Decoupling four-fermion terms using Eq. (25), we obtain the quadratic Hamiltonian in the form  $H_{\text{eff}}^{(2)} = H^{\text{kin}} + H_{\alpha_1\beta}^{(2)} + H_{\alpha_2\beta}^{(2)}$ , where

$$H^{\text{kin}} = \sum_{\mathbf{p}, \sigma, i=1,2} \varepsilon_{\mathbf{p}} [\alpha_{i\mathbf{p}\sigma}^\dagger \alpha_{i\mathbf{p}\sigma} - \beta_{i\mathbf{p}\sigma}^\dagger \beta_{i\mathbf{p}\sigma}], \quad (26)$$

$$\begin{aligned}H_{\alpha_1\beta}^{(2)} &= - \sum_{\mathbf{p}} [\alpha_{1\mathbf{p}\uparrow}^\dagger (\Delta_1^z \beta_{1\mathbf{p}\uparrow} + \Delta_2^x \beta_{2\mathbf{p}\downarrow}) \\ &\quad - \alpha_{1\mathbf{p}\downarrow}^\dagger (\Delta_1^z \beta_{1\mathbf{p}\downarrow} - \Delta_2^x \beta_{2\mathbf{p}\uparrow})] + \text{H.c.},\end{aligned}$$

$$\begin{aligned}H_{\alpha_2\beta}^{(2)} &= - \sum_{\mathbf{p}} [\alpha_{2\mathbf{p}\uparrow}^\dagger (\Delta_3^z \beta_{1\mathbf{p}\uparrow} + \Delta_4^x \beta_{2\mathbf{p}\downarrow}) \\ &\quad - \alpha_{2\mathbf{p}\downarrow}^\dagger (\Delta_3^z \beta_{1\mathbf{p}\downarrow} - \Delta_4^x \beta_{2\mathbf{p}\uparrow})] + \text{H.c.}\end{aligned}\quad (27)$$

The part involving  $\alpha_1$  hole band and  $\Delta_1^z$  and  $\Delta_1^x$  can be diagonalized in the same way as for the three-band model, by introducing  $\cos \theta = \Delta_1^z / \Delta_1$  and  $\sin \theta = \Delta_1^x / \Delta_1$ , where  $\Delta_1 = \sqrt{(\Delta_1^z)^2 + (\Delta_1^x)^2}$  and rotating  $\beta_{1,2}$  into

$$\begin{aligned}\beta_{1\mathbf{p}\downarrow} &= c_{b\mathbf{p}} \cos \theta - d_{b\mathbf{p}} \sin \theta, \\ \beta_{2\mathbf{p}\downarrow} &= c_{a\mathbf{p}} \sin \theta + d_{a\mathbf{p}} \cos \theta, \\ \beta_{1\mathbf{p}\uparrow} &= c_{a\mathbf{p}} \cos \theta - d_{a\mathbf{p}} \sin \theta, \\ \beta_{2\mathbf{p}\uparrow} &= -c_{b\mathbf{p}} \sin \theta - d_{b\mathbf{p}} \cos \theta.\end{aligned}\quad (28)$$

Substituting this into Eq. (26) we obtain

$$H_{\alpha_1\beta}^{(2)} = -\Delta_1 \sum_{\mathbf{p}} [\alpha_{1\mathbf{p}\uparrow}^\dagger c_{a\mathbf{p}} - \alpha_{1\mathbf{p}\downarrow}^\dagger c_{b\mathbf{p}}] \quad (29)$$

and  $H^{\text{kin}} = H_{\{\alpha_1, c\}}^{\text{kin}} + H_{\{\alpha_2, d\}}^{\text{kin}}$ , where

$$H_{\{\alpha_1, c\}}^{\text{kin}} = \sum_{\mathbf{p}} \varepsilon_{\mathbf{p}} [\alpha_{1\mathbf{p}\uparrow}^\dagger \alpha_{1\mathbf{p}\uparrow} + \alpha_{1\mathbf{p}\downarrow}^\dagger \alpha_{1\mathbf{p}\downarrow} - c_{a\mathbf{p}}^\dagger c_{a\mathbf{p}} - c_{b\mathbf{p}}^\dagger c_{b\mathbf{p}}], \quad (30)$$

$$H_{\{\alpha_2, d\}}^{\text{kin}} = \sum_{\mathbf{p}} \varepsilon_{\mathbf{p}} [\alpha_{2\mathbf{p}\uparrow}^\dagger \alpha_{2\mathbf{p}\uparrow} + \alpha_{2\mathbf{p}\downarrow}^\dagger \alpha_{2\mathbf{p}\downarrow} - d_{a\mathbf{p}}^\dagger d_{a\mathbf{p}} - d_{b\mathbf{p}}^\dagger d_{b\mathbf{p}}]. \quad (31)$$

The part  $H_{\{\alpha_1, c\}}^{\text{kin}} + H_{\alpha_1\beta}^{(2)}$  involves hole  $\alpha_1$  operators and electron  $c_{a,b}$  operators

$$\begin{aligned}H_{\{\alpha_1, c\}}^{\text{kin}} + H_{\alpha_1\beta}^{(2)} &= \sum_{\mathbf{p}} \varepsilon_{\mathbf{p}} [\alpha_{1\mathbf{p}\uparrow}^\dagger \alpha_{1\mathbf{p}\uparrow} + \alpha_{1\mathbf{p}\downarrow}^\dagger \alpha_{1\mathbf{p}\downarrow} - c_{a\mathbf{p}}^\dagger c_{a\mathbf{p}} - c_{b\mathbf{p}}^\dagger c_{b\mathbf{p}}] \\ &\quad - \Delta_1 \sum_{\mathbf{p}} [\alpha_{1\mathbf{p}\uparrow}^\dagger c_{a\mathbf{p}} - \alpha_{1\mathbf{p}\downarrow}^\dagger c_{b\mathbf{p}}].\end{aligned}\quad (32)$$

Equation (32) can be diagonalized by the same transformation as in Eqs. (6) and (7)

$$\begin{aligned}\alpha_{1\mathbf{p}\uparrow} &= p_{a\mathbf{p}} \cos \psi + e_{a\mathbf{p}} \sin \psi, \\ c_{a\mathbf{p}} &= e_{a\mathbf{p}} \cos \psi - p_{a\mathbf{p}} \sin \psi, \\ \alpha_{1\mathbf{p}\downarrow} &= p_{b\mathbf{p}} \cos \tilde{\psi} + e_{b\mathbf{p}} \sin \tilde{\psi}, \\ c_{b\mathbf{p}} &= e_{b\mathbf{p}} \cos \tilde{\psi} - p_{b\mathbf{p}} \sin \tilde{\psi},\end{aligned}\quad (33)$$

where, as before,  $\tilde{\psi} = \frac{\pi}{2} + \psi$  and  $\cos^2 \psi$ ,  $\sin^2 \psi = \frac{1}{2} [1 \pm \frac{\varepsilon_{\mathbf{p}}}{\sqrt{(\varepsilon_{\mathbf{p}})^2 + \Delta_1^2}}]$ . Substituting, we obtain

$$H_{\{\alpha_1, c\}}^{\text{kin}} + H_{\alpha_1\beta}^{(2)} = \sum_{\mathbf{p}} E_{1,\mathbf{p}} [e_{a\mathbf{p}}^\dagger e_{a\mathbf{p}} + p_{b\mathbf{p}}^\dagger p_{b\mathbf{p}} - e_{b\mathbf{p}}^\dagger e_{b\mathbf{p}} - p_{a\mathbf{p}}^\dagger p_{a\mathbf{p}}], \quad (34)$$

where  $E_{1,\mathbf{p}} = \pm \sqrt{(\varepsilon_{\mathbf{p}})^2 + \Delta_1^2}$ . This result is similar to Eq. (8). The self-consistent equation for the gap  $\Delta_1$  is



$$1 = \frac{U_{\text{SDW}}^{(1)}}{2N} \sum_{\mathbf{p}} \frac{1}{\sqrt{(\varepsilon_{\mathbf{p}})^2 + \Delta_1^2}}. \quad (35)$$

The remaining part of the Hamiltonian involves holes from  $\alpha_2$  band and reduces to

$$\begin{aligned} H_{\{\alpha_2, d\}}^{\text{kin}} + H_{\alpha_2 \beta}^{(2)} = & \sum_{\mathbf{p}} \varepsilon_{\mathbf{p}} [\alpha_{2\mathbf{p}\uparrow}^\dagger \alpha_{2\mathbf{p}\uparrow} + \alpha_{2\mathbf{p}\downarrow}^\dagger \alpha_{2\mathbf{p}\downarrow} - d_{\mathbf{ap}}^\dagger d_{\mathbf{ap}} \\ & - d_{b\mathbf{p}}^\dagger d_{b\mathbf{p}}] - \Delta_2 [\alpha_{2\mathbf{p}\uparrow}^\dagger [c_{a,\mathbf{p}} \cos(\tilde{\theta} - \theta) \\ & + d_{a,\mathbf{p}} \sin(\tilde{\theta} - \theta)] - \alpha_{2\mathbf{p}\downarrow}^\dagger [c_{a,\mathbf{p}} \cos(\tilde{\theta} - \theta) \\ & + d_{a,\mathbf{p}} \sin(\tilde{\theta} - \theta)]], \end{aligned} \quad (36)$$

where we introduced  $\cos \tilde{\theta} = \Delta_2^z / \Delta_2$ ,  $\sin \tilde{\theta} = \Delta_2^x / \Delta_2$ , and  $\Delta_2 = \sqrt{(\Delta_2^z)^2 + (\Delta_2^x)^2}$ .

This part of the Hamiltonian decouples from the one which we already diagonalized if we eliminate the terms with  $c$  operators. This will be the case if we choose  $\tilde{\theta} = \pi/2 + \theta$ . Then Eq. (36) becomes the quadratic form of hole  $\alpha_2$  operators and electron  $d_{a,b}$  operators neither of which is present in the quadratic form of Eq. (32). Diagonalizing the quadratic form in Eq. (36), we obtain, in terms of new operators  $\tilde{e}_{a,b}$  and  $\tilde{p}_{a,b}$

$$H_{\{\alpha_2, d\}}^{\text{kin}} + H_{\alpha_2 \beta}^{(2)} = \sum_{\mathbf{p}} E_{2,\mathbf{p}} [\tilde{e}_{a\mathbf{p}}^\dagger \tilde{e}_{a\mathbf{p}} + \tilde{p}_{b\mathbf{p}}^\dagger \tilde{p}_{b\mathbf{p}} - \tilde{e}_{b\mathbf{p}}^\dagger \tilde{e}_{b\mathbf{p}} - \tilde{p}_{a\mathbf{p}}^\dagger \tilde{p}_{a\mathbf{p}}], \quad (37)$$

where  $E_{2,\mathbf{p}} = \pm \sqrt{(\varepsilon_{\mathbf{p}})^2 + \Delta_2^2}$ . The self-consistent equation for the gap  $\Delta_2$  is

$$1 = \frac{U_{\text{SDW}}^{(2)}}{2N} \sum_{\mathbf{p}} \frac{1}{\sqrt{(\varepsilon_{\mathbf{p}})^2 + \Delta_2^2}}. \quad (38)$$

We see that, by choosing  $\tilde{\theta} = \pi/2 - \theta$ , we decoupled the quadratic form into two parts, one for  $\Delta_1$ , another for  $\Delta_2$ . One can easily check that for both parts it is energetically favorable to have a state with nonzero  $\Delta$  once self-consistent equations for  $\Delta_{1,2}$  have solutions. This implies that the energy is further reduced if, in addition to creating  $\Delta_1^z = \Delta_1 \cos \theta$  and  $\Delta_1^x = \Delta_1 \sin \theta$ , one also creates  $\Delta_2^z = -\Delta_2 \sin \theta$  and  $\Delta_2^x = \Delta_2 \cos \theta$ . Furthermore, for equal-size circular FSs, the solutions for  $\Delta_1$  and  $\Delta_2$  exist for any  $U_{\text{SDW}}^{(1)}$  and  $U_{\text{SDW}}^{(2)}$ . The resulting fermionic excitations are fully gapped, i.e., within four-band model of equal-size circular hole and electron pockets, an SDW state is an insulator.

We now verify whether such insulating state is consistent with the observed  $(0, \pi)$  or  $(\pi, 0)$  order. Because the angle  $\theta$  disappears from the quadratic forms in Eq. (32) and (36) (for  $\tilde{\theta} = \pi/2 - \theta$ ), the ground state is again degenerate. The degenerate SDW OP manifold is given by

$$\begin{aligned} \tilde{S}(\mathbf{R}) \propto & \tilde{n}_z (\Delta_1 \cos \theta - \Delta_2 \sin \theta) e^{i\mathbf{Q}_1 \mathbf{R}} \\ & + \tilde{n}_x (\Delta_1 \sin \theta + \Delta_2 \cos \theta) e^{i\mathbf{Q}_2 \mathbf{R}}. \end{aligned} \quad (39)$$

This degenerate set does contain  $(0, \pi)$  and  $(\pi, 0)$  states with only one ordering vector (either  $\mathbf{Q}_1$  or  $\mathbf{Q}_2$ ). These states are obtained if we set  $\tan \theta = \Delta_1 / \Delta_2$  or  $\tan \theta = -\Delta_2 / \Delta_1$ . The issue

then is whether such states are selected by other interactions in the same spirit as  $(0, \pi)$  or  $(\pi, 0)$  orders were selected in the three-band model. We argue that they are not. The argument is that  $(0, \pi)$  and  $(\pi, 0)$  ordered states in the four-band model are obtained by choosing  $\theta$  such that  $\tilde{\Delta}_1$  and  $\tilde{\Delta}_2$  have components with both momenta,  $\mathbf{Q}_1$  and  $\mathbf{Q}_2$ . The total spin component with either  $\mathbf{Q}_1$  or  $\mathbf{Q}_2$  vanishes because of cancellation between  $\Delta_1$  and  $\Delta_2$  components. Indeed, for  $U_{\text{SDW}}^{(2)} \ll U_{\text{SDW}}^{(1)}$   $\theta$  is close to zero or to  $\pi/2$  but it is not equal to either of these values. Meanwhile, when we considered lifting of the degeneracy in the three-band model, we found that the interactions between  $\beta_1$  and  $\beta_2$  electrons and the ellipticity give rise to the  $\theta$  dependence of  $E_{gr}$  in the form  $E_{gr}(\theta) = E_0 + E_1 \sin^2(2\theta)$  such that  $E_{gr}(\theta)$  has minima at  $\theta$  exactly equal to 0 or to  $\pi/2$ . To verify what happens in the four-band model, we extended those calculations to the case when  $U_{\text{SDW}}^{(2)}$  is nonzero and analyzed the form of  $E_{gr}(\theta)$  perturbatively in  $U_{\text{SDW}}^{(2)} / U_{\text{SDW}}^{(1)}$ . We skip the details of the calculations as they are similar to the ones for the three-band model. We found that the minima in  $E_{gr}(\theta)$  do not shift from  $\theta=0$  and  $\theta=\pi/2$ , at least at small  $U_{\text{SDW}}^{(2)} / U_{\text{SDW}}^{(1)}$ . The consequence is that, for the four-band model, interactions which break the degeneracy of SDW manifold favor the states which are not  $(0, \pi)$  or  $(\pi, 0)$  states. For example, when  $\theta=0$ ,  $\tilde{S}(\mathbf{R}) \propto \Delta_1 \tilde{n}_z e^{i\mathbf{Q}_1 \mathbf{R}} + \Delta_2 \tilde{n}_x e^{i\mathbf{Q}_2 \mathbf{R}}$ . Such SDW state is a two-sublattice structure with equal magnitudes of the order parameters on the two sublattices but with a noncollinear spin order.

The outcome of this study is that  $(0, \pi)$  or  $(\pi, 0)$  order can only be preserved if  $\Delta_2$  is strictly zero, i.e., the second hole band is not involved in the SDW mixing. Only then interactions and ellipticity select  $(0, \pi)$  or  $(\pi, 0)$  states. Otherwise, the order necessary has both  $\mathbf{Q}_1$  and  $\mathbf{Q}_2$  components and the SDW OP has modulations along both  $x$  and  $y$  directions.

This observation has an implication for the electronic structure. When  $\Delta_2=0$ , one hole band and one electron band are not involved in the SDW mixing, i.e., the system *remains a metal even when SDW mixing of the other two bands is strong*. In other words,  $(0, \pi)$  and  $(\pi, 0)$  SDW order necessary involves only one of two hole bands and only one of the two electron bands. The other hole and electron bands remain intact.

As we said, for equal-size circular hole and electron pockets, there is a perfect nesting between both primary and secondary pairs of hole and electron states, and  $\Delta_2$  is nonzero for any nonzero  $U_{\text{SDW}}^{(2)}$ . This is, however, not the case when the two hole FSs are circles of unequal size and the two electron FSs are ellipses. In this situation, redoing the same calculations as above we obtain in general four different SDW bands described by

$$\begin{aligned} H_{\text{SDW}} = & \sum_{a,b} \sum_{\mathbf{p}} E_{1,2\mathbf{p}} (e_{a,b\mathbf{p}}^\dagger e_{a,b\mathbf{p}} + p_{b,a\mathbf{p}}^\dagger p_{b,a\mathbf{p}}) \\ & + E_{3,4\mathbf{p}} (e_{a,b\mathbf{p}}^\dagger e_{a,b\mathbf{p}} + p_{b,a\mathbf{p}}^\dagger p_{b,a\mathbf{p}}). \end{aligned} \quad (40)$$

Here

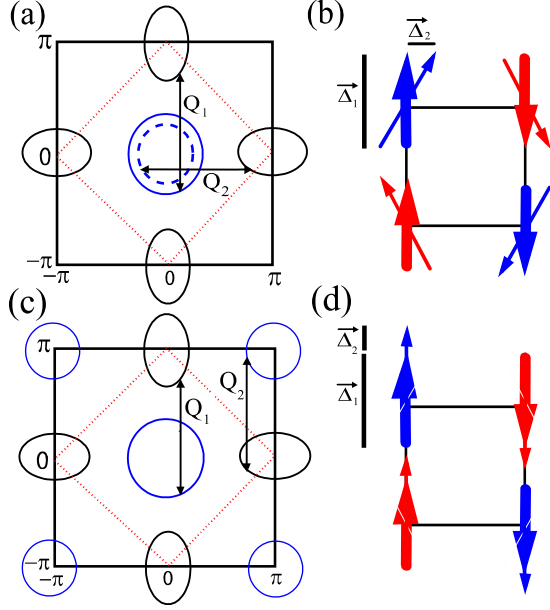


FIG. 4. (Color online) The changes to the magnetic structure introduced by the weak SDW coupling  $\tilde{\Delta}_2$  between the second hole band and the electron bands. Panels (a) and (b) are for the FS topology of the pnictides, panels (c) and (d) are for the FS topology of  $t'$ - $t$  model for  $t \ll t'$ .

$$E_{1,2\mathbf{p}} = \frac{1}{2}(\varepsilon_{\mathbf{p}}^{\alpha_1} + \tilde{\varepsilon}_{\mathbf{p}}) \pm \frac{1}{2}\sqrt{(\varepsilon_{\mathbf{p}}^{\alpha_1} - \tilde{\varepsilon}_{\mathbf{p}})^2 + 4|\Delta_1|^2} \quad (41)$$

and

$$E_{3,4\mathbf{p}} = \frac{1}{2}(\varepsilon_{\mathbf{p}}^{\alpha_2} + \tilde{\varepsilon}_{\mathbf{p}}) \pm \frac{1}{2}\sqrt{(\varepsilon_{\mathbf{p}}^{\alpha_2} - \tilde{\varepsilon}_{\mathbf{p}})^2 + 4|\Delta_2|^2}, \quad (42)$$

where  $\tilde{\varepsilon}_{\mathbf{p}} = \varepsilon_{\mathbf{p}}^{\beta_1} \cos^2 \theta + \varepsilon_{\mathbf{p}}^{\beta_2} \sin^2 \theta$  and  $\tilde{\varepsilon}_{\mathbf{p}} = \varepsilon_{\mathbf{p}}^{\beta_2} \cos^2 \theta + \varepsilon_{\mathbf{p}}^{\beta_1} \sin^2 \theta$ . The self-consistent equations for the two gaps are

$$1 = U_{\text{SDW}}^{(1)} \sum_{\mathbf{p}} \frac{n(E_{1\mathbf{p}}) - n(E_{2\mathbf{p}})}{\sqrt{(\varepsilon_{\mathbf{k}}^{\alpha_1} - \tilde{\varepsilon}_{\mathbf{k}})^2 + 4|\Delta_1|^2}}, \quad (43)$$

$$1 = U_{\text{SDW}}^{(2)} \sum_{\mathbf{p}} \frac{n(E_{3\mathbf{p}}) - n(E_{4\mathbf{p}})}{\sqrt{(\varepsilon_{\mathbf{k}}^{\alpha_2} - \tilde{\varepsilon}_{\mathbf{k}})^2 + 4|\Delta_2|^2}}. \quad (44)$$

Analyzing these equations, we found that, for a nonperfect nesting, SDW magnetism is a threshold phenomenon, i.e., to obtain a nonzero  $\Delta_1$  and  $\Delta_2$ , the interactions  $U_{\text{SDW}}$  must exceed the thresholds. We found that a hole band with a heavier mass, e.g., with a *larger* FS, is more strongly coupled to electron bands. This band then plays the role of the  $\alpha_1$  band in our theory. Once the corresponding  $U_{\text{SDW}}^{(1)}$  exceeds the threshold value  $U_{\text{cr}}^{(1)}$ , the system develops an SDW order ( $\Delta_1 \neq 0$ ). This order, as we know, is a stripe  $(0, \pi)$  or  $(\pi, 0)$  order. For the smaller-size hole band ( $\alpha_2$  band in our terminology), SDW order with  $\Delta_2 \neq 0$  emerges only when  $U_{\text{SDW}}^{(2)}$  exceeds a larger threshold  $U_{\text{cr}}^{(2)} > U_{\text{cr}}^{(1)}$ . Once this happens, SDW order acquires both  $\mathbf{Q}_1$  and  $\mathbf{Q}_2$  components. This is illustrated in Figs. 4(a) and 4(b). We see therefore that the

regime consistent with the experiments is  $U_{\text{SDW}}^{(1)} > U_{\text{cr}}^{(1)}$  and  $U_{\text{SDW}}^{(2)} < U_{\text{cr}}^{(2)}$ . This regime is quite realistic given that there is quite sizable difference between the areas of the two hole pockets.

#### $t$ - $t'$ - $U$ model

In simple terms, our result that the stripe order is only consistent with  $\Delta_1 \neq 0$ ,  $\Delta_2 = 0$  is ultimately related to the geometry of the FS, namely, to the fact that both hole FSs are located around the  $\Gamma$  point. Indeed, suppose that one hole and one electron FSs are mixed into an SDW state with the momenta between these FSs (say  $[\mathbf{Q}_1 = (0, \pi)]$ ). For strong interaction, the SDW excitations are gapped and effectively decouple from the other hole and electron bands. These two bands can also mix into an SDW state, however, because the second hole band is centered at  $(0, 0)$ , it is separated from the second electron band by  $\mathbf{Q}_2 = (\pi, 0)$ , i.e., the second SDW order necessary has momentum  $(\pi, 0)$ , and the stripe order gets broken.

The SDW order would be different if the second FS was centered at  $(\pi, \pi)$  because then the remaining hole and electron bands would be separated by the same  $\mathbf{Q}$  as the first pair of bands, and the stripe configuration would not be broken by the emergence of the second SDW order. This is illustrated in Figs. 4(c) and 4(d).

Such FS geometry is realized in the half-filled  $t$ - $t'$ - $U$  model described by

$$H = t \sum_{i, \delta_1 \sigma} c_{i\sigma}^\dagger c_{i+\delta_1 \sigma} + t' \sum_{i, \delta_2 \sigma} c_{i\sigma}^\dagger c_{i+\delta_2 \sigma} + U \sum_i n_{i\uparrow} n_{i\downarrow}, \quad (45)$$

where  $\delta_1$  and  $\delta_2$  are distances to nearest and next-nearest neighbors, and  $n_{i\sigma} = c_{i\sigma}^\dagger c_{i\sigma}$ . In momentum space, the dispersion  $\varepsilon_{\mathbf{p}} = 2t(\cos p_x + \cos p_y) + 4t' \cos p_x \cos p_y - \mu$  has maxima at  $(0, 0)$  and  $(\pi, \pi)$  and isotropic quadratic holelike dispersion around these points [with nonequal masses near  $(0, 0)$  and  $(\pi, \pi)$ , when  $t \neq 0$ ], and minima at  $(0, \pi)$  and  $(\pi, 0)$  and elliptical electronlike dispersion near these points. We illustrate this in Fig. 5. Such band structure is topologically equivalent to the one shown in Fig. 4(c).

At large  $U$ , the  $t$ - $t'$ - $U$  model reduces by standard manipulations to the  $J_1$ - $J_2$  Heisenberg spin model. The electronic states in this model are all gapped, and the SDW OP is degenerate at the mean-field level. We analyzed SDW order in the  $t$ - $t'$ - $U$  model for arbitrary  $U$  within the same computational scheme as before and found that  $(0, \pi)$  and  $(\pi, 0)$  states minimize the energy at the mean-field level because both  $\tilde{\Delta}_1$  and  $\tilde{\Delta}_2$  appear with the same momentum.

It is instructive to consider the discrepancy between our four-band model and  $t$ - $t'$ - $U$  model is some more detail. We remind that in our model, ellipticity of electron pockets and interactions between them select  $(0, \pi)$  and  $(\pi, 0)$  states already at the mean-field level. We show below that in  $t$ - $t'$ - $U$  model there is no selection of a particular SDW order at the mean-field level even when  $t \neq 0$  and electron dispersion is elliptical. In this situation,  $(0, \pi)$  and  $(\pi, 0)$  states remain degenerate with infinite number of other two-sublattice states. Beyond mean-field level, quantum fluctuations select  $(0, \pi)$  or  $(\pi, 0)$  order in the  $J_1$ - $J_2$  model. We haven't check

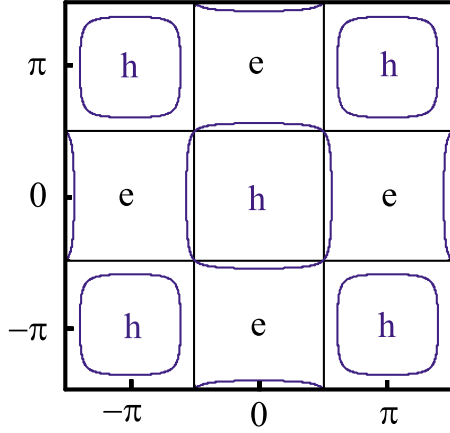


FIG. 5. (Color online) The FS for the tight-binding model  $\varepsilon_{\mathbf{p}} = 4t' \cos p_x \cos p_y + 2t(\cos p_x + \cos p_y)$  for  $t=0$  (squares) and  $t=0.5t'$  (curves).  $h$  and  $e$  refer to the hole and electron states occupying the corresponding parts of the BZ. Observe that the hole bands are now centered at  $(0,0)$  and  $(\pi,\pi)$ .

the selection of the SDW order at smaller  $U$  but it is likely that  $(0,\pi)$  and  $(\pi,0)$  states are selected for all values of  $U$ .

To demonstrate that mean-field SDW OP in  $t$ - $t'$ - $U$  model remains degenerate, consider this model at small  $t$  and introduce two SDW order parameters  $\vec{\Delta}_1 = -(U/2N) \sum_{\mathbf{k}} \langle c_{\mathbf{k},\alpha}^\dagger \sigma_{\alpha\beta} c_{\mathbf{k}+\mathbf{Q}_1,\beta} \rangle$  with momentum  $\mathbf{Q}_1$  and  $\vec{\Delta}_2 = -(U/2N) \sum_{\mathbf{k}} \langle c_{\mathbf{k},\alpha}^\dagger \sigma_{\alpha\beta} c_{\mathbf{k}+\mathbf{Q}_2,\beta} \rangle$  with momentum  $\mathbf{Q}_2$ . We introduce four fermionic operators with momenta near  $(0,0)$ ,  $(0,\pi)$ ,  $(\pi,0)$ , and  $(\pi,\pi)$ , and re-express  $t$ - $t'$ - $U$  model as the model of holes and electrons. We skip computational details, which are not different from what we presented in previous sections and only cite the results. The extra terms in the quadratic form come from the interactions between holes and electrons. For  $t=0$ , all four dispersions are equal (up to the overall sign), and the Hamiltonian is diagonalized in the same way as in Sec. II B. Not surprising, the ground-state energy depends only on  $(\Delta_1)^2 + (\Delta_2)^2$ , i.e., there exists a degenerate manifold of SDW OPs.

Consider next the effect of the interactions between the electron bands. There are four effective electron-electron interactions—the analogs of  $U_6$ ,  $U_7$ ,  $U_8$ , and  $U_4$  in Eq. (10). They all originate from the same  $U$  term and have the same prefactors. According to Eq. (12), the extra term in the ground-state energy from electron-electron interaction only has  $(\vec{\Delta}_1 \cdot \vec{\Delta}_2)^2$  part

$$E_{gr}^{ex} = 4A^2 U \frac{(\vec{\Delta}_1 \cdot \vec{\Delta}_2)^2}{\Delta^4}. \quad (46)$$

This term orders  $\vec{\Delta}_1$  and  $\vec{\Delta}_2$  perpendicular to each other, what makes the magnitudes of the two sublattice OPs  $\vec{\Delta}_1 + \vec{\Delta}_2$  and  $\vec{\Delta}_1 - \vec{\Delta}_2$  equal. But in the absence of  $|\vec{\Delta}_1|^2 \cdot |\vec{\Delta}_2|^2$  term, the angle between the two sublattices remains arbitrary.

Consider next the effect of ellipticity of electron pockets. In our model, we remind, ellipticity gave rise to two contributions to  $E_{gr}$ , both scale as  $|\vec{\Delta}_1|^2 \cdot |\vec{\Delta}_2|^2$ . The two contributions were of opposite sign but were not equal. In  $t$ - $t'$ - $U$

model, the situation is very similar—there are again two contributions to  $E_{gr}$ : one is the second-order contribution from nondiagonal terms in the Hamiltonian, induced by  $t$ , another comes from the change in the dispersion of the diagonal terms. The contribution from nondiagonal terms is given by

$$E_{gr}^{a,ellipt} = 8t^2 \frac{|\vec{\Delta}_1|^2 |\vec{\Delta}_2|^2}{\Delta^4} \times \sum_{\mathbf{p}} \frac{(\cos^2 p_x + \cos^2 p_y) \Delta^2}{[\Delta^2 + 16(t')^2 \cos^2 p_x \cos^2 p_y]^{3/2}} + \dots, \quad (47)$$

where, as before, the dots stand for the terms which depend only on  $\Delta$ . The contribution from the change in the dispersion of the diagonal terms in the Hamiltonian is

$$E_{gr}^{b,ellipt} = 2 \sum_{\mathbf{p}} \left[ \varepsilon_{c1} + \varepsilon_{c2} + \varepsilon_{fa} + \varepsilon_{fb} - \sqrt{\left( \frac{\varepsilon_{c1} + \varepsilon_{fa}}{2} \right)^2 + \Delta^2} - \sqrt{\left( \frac{\varepsilon_{c2} + \varepsilon_{fb}}{2} \right)^2 + \Delta^2} \right], \quad (48)$$

where

$$\varepsilon_{c1} = 4t' \cos p_x \cos p_y + 2t(\cos p_x + \cos p_y),$$

$$\varepsilon_{c2} = 4t' \cos p_x \cos p_y - 2t(\cos p_x + \cos p_y),$$

$$\varepsilon_{fa} = -4t' \cos p_x \cos p_y + 2t(\cos p_x + \cos p_y) \left( \frac{\vec{\Delta}_1^2 - \vec{\Delta}_2^2}{\Delta^2} \right),$$

$$\varepsilon_{fb} = -4t' \cos p_x \cos p_y - 2t(\cos p_x + \cos p_y) \left( \frac{\vec{\Delta}_1^2 - \vec{\Delta}_2^2}{\Delta^2} \right). \quad (49)$$

Substituting these energies into Eq. (48) and expanding in  $t$ , we find

$$E_{gr}^{b,ellipt} = -8t^2 \frac{|\vec{\Delta}_1|^2 |\vec{\Delta}_2|^2}{\Delta^4}, \quad \sum_{\mathbf{p}} \frac{(\cos^2 p_x + \cos^2 p_y) \Delta^2}{[\Delta^2 + 16(t')^2 \cos^2 p_x \cos^2 p_y]^{3/2}} + \dots \quad (50)$$

Comparing Eqs. (47) and (50), we find that  $E_{gr}^{a,ellipt} + E_{gr}^{b,ellipt} = 0$ , i.e., ellipticity of electron bands in  $t$ - $t'$ - $U$  model does not give rise to a selection of a particular SDW OP from the degenerate manifold. This result very likely holds for arbitrary  $t/t'$ , as long as the ground-state manifold consists of states with antiferromagnetic order along the diagonals.

#### IV. ELECTRONIC STRUCTURE OF THE SDW STATE

As we said earlier, when all four Fermi surfaces are circles of equal size, all four Fermi surfaces are mixed by the SDW and are gapped. However, as soon as the two hole pockets become nonequal, there is a range of the interactions when one hole pocket and one of the two electron pockets

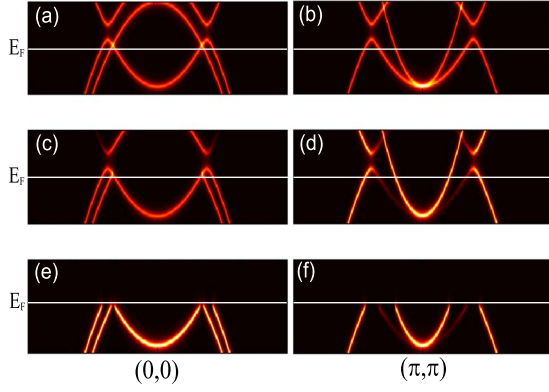


FIG. 6. (Color online) Calculated image of the electronic structure in the folded BZ in the SDW phase. Left panel—near  $\Gamma = (0,0)$  and right panel—near  $M = (\pi, \pi)$ . In figures (a) and (b) we show the dispersion, in figures (c) and (d) the spectral function  $\text{Im } G(\mathbf{k}, \omega) = \sum_i \text{Im } G_i$ , and in figures (e) and (f) ARPES intensity, i.e., the product  $\text{Im } G(\mathbf{k}, \omega) \times n_F(E_{\mathbf{k}})$ . The direction of momenta in all figures is along  $k_x = k_y$  in the folded BZ. We directed SDW order parameter along  $z$  axis and set  $\Delta_1^z \neq 0$ ,  $\Delta_2 = \Delta_3 = \Delta_4 = 0$  [(0,  $\pi$ ) order]. For definiteness we set  $\Delta_1^z = \mu/4$ ,  $\mu_1 = (3/2)\mu$ ,  $\mu_2 = (3/2)\mu$ , and  $m_1 = m_2 = m_y = 2m_x = 1$ . For numerical purposes we added the small damping constant  $\delta = 0.04\mu$ .

are mixed by SDW but the other hole and electron pockets remain intact. As a consequence, in the folded BZ, to which the experimental data refer to, the electronic structure contains one hole and one electron band mixed by SDW order and visible both near (0,0) and  $(\pi, \pi)$ , one hole band visible only near (0,0), and one electron band visible only near  $(\pi, \pi)$ . The only effect of SDW ordering on the nonmixed excitations is the  $\Delta$  dependence of the intensity via coherence factors. Besides, for moderately strong interactions, as in the pnictides,  $\Delta_1$  is not too large, and the SDW-mixed dispersions form the new FSs.<sup>33</sup> The net result is the presence of three bands near the  $\Gamma$  point, one of which (the hole band) is not modified by SDW, and another three bands close to the  $(\pi, \pi)$  point, one of which (the electron band) is not modified by SDW [see Figs. 6(a) and 6(b)].

The spectral functions  $\sum_i \text{Im } G_i$  are peaked at quasiparticle energies but are also sensitive, via the SDW coherence factors, to the interplay between the effective masses of the bare hole and electron dispersions. For example, for two equivalent hole pockets ( $m_1 = m_2$ ) and  $m_x < m_1 = m_y$ , the spectral weight of ARPES intensity  $\sum_i n_F(E_{\mathbf{k}_i}) \times \text{Im } G_i$  [ $n_F(E)$  is a Fermi function], which we plot in Figs. 6(e) and 6(f), is the largest for two holelike bands centered around  $\Gamma$  point, and for one electron band and hole “half bands” (hole blades) around  $(\pi, \pi)$  point. This theoretical ARPES intensity is quite consistent with the experimental data from Refs. 25–27: the experiments also show two hole dispersions near  $\Gamma$  point, and one electron band and two hole half bands near  $(\pi, \pi)$ . There is some evidence<sup>26</sup> of the third hole dispersion near (0,0) but this one likely emerges from the fifth band which we did not consider here.

Our results are also consistent with recent observations of “anisotropic Dirac cones.”<sup>40,41</sup> Indeed, the bands mixed in the SDW state form small hole pockets near both  $\Gamma$  and  $M$

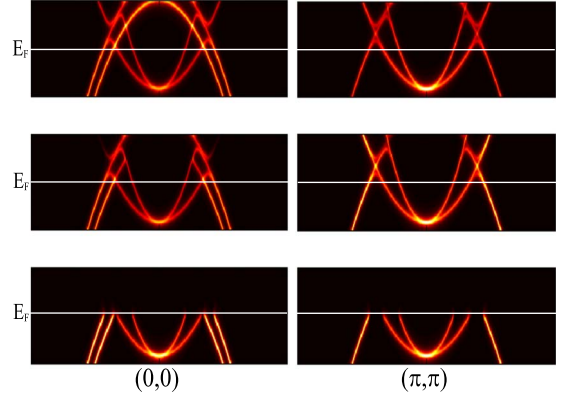


FIG. 7. (Color online) Same as in Fig. 6 but for a multidomain sample with equal distribution of the domains with  $(\pi, 0)$  and  $(0, \pi)$  SDW orders.

points of the BZ, and the dispersion around these pockets is almost linear close to the Fermi level and also anisotropic between  $k_x$  and  $k_y$  due to initial anisotropy of the elliptic band involved in the SDW mixing. However, despite of a visual similarity with the Dirac cone, the dispersion is still quadratic near the top of the hole band. There is also an “accidental” Dirac cone in Fig. 6 near the  $\Gamma$  point, at a momentum where the dispersion of the SDW-mixed band intersects with that of the hole band which does not participate in the SDW mixing. This intersection need not to be at the FS but occurs close to the FS for the parameters chosen in Fig. 6.

In Fig. 6 we assumed that a particular SDW order [(0,  $\pi$ ) in that figure] is the same in the whole sample. It is quite possible, though, that the system has domains with  $(\pi, 0)$  and  $(0, \pi)$  orders. This idea has been recently put forward in Ref. 28. In Fig. 7 we show the dispersions, the spectral functions, and the ARPES intensities for a multidomain sample, assuming equal distributions of the domains with  $(\pi, 0)$  and  $(0, \pi)$  orders. Comparing Figs. 6 and 7, we clearly see that main effect of averaging over two different SDW orders is the appearance of an additional electron dispersion near the  $M$  point. This second electron dispersion is consistent with recent ARPES measurements of the electronic structure in  $\text{BaFe}_2\text{As}_2$  by Shen and co-workers.<sup>28</sup>

## V. SUMMARY

To summarize, in this paper we analyzed SDW order in the itinerant model for Fe pnictides. We considered a model consisting of two hole bands centered at (0,0) and two electron bands centered at (0,  $\pi$ ) and  $(\pi, 0)$  points in the unfolded BZ [in the folded zone, this corresponds to two hole bands centered at (0,0) and two electron bands centered at  $(\pi, \pi)$ ].

We assumed that one hole band is more strongly coupled to electron bands and considered first a three-band model consisting of one hole and two electron bands. We found that SDW order in this model is highly degenerate for the case of a perfect nesting and if we restrict with only the interactions between holes and electrons which give rise to a SDW insta-



bility. The degeneracy of the SDW order parameter is due to the fact that the energy gain to create SDW order parameters with momentum  $\mathbf{Q}_1=(0, \pi)$  or  $\mathbf{Q}_2=(\pi, 0)$  is the same. The order-parameter manifold consists of states with a perfect antiferromagnetic order along diagonals but with nonequal values and arbitrary directions of the OPs at nearest neighbors.

We demonstrated that the degeneracy is broken once we include into consideration interactions between two electron pockets and ellipticity of these pockets. Both the interactions and the ellipticity select  $(0, \pi)$  or  $(\pi, 0)$  stripe phases with only one ordering momenta, either  $\mathbf{Q}_1$  or  $\mathbf{Q}_2$ . These stripe-ordered states are in agreement with the experiments on FeAs-based pnictides. The selection of either  $(0, \pi)$  or  $(\pi, 0)$  order leaves one electron FS intact and the system remains a metal even when SDW order is strong, and the two bands involved in the SDW mixing are fully gapped.

We argued that the selection of stripe states only occurs when the interaction between electron pockets is in the charge channel. We considered, as an example, the model with the interaction in the spin channel and showed that there electron-electron interactions select a different state.

We next added the second hole band and argued that it mixes with the electron band which was left out of the SDW mixing in the three-band model, once the corresponding coupling exceeds the critical value. We found, however, that this second SDW order necessary gives rise to a nonstripe spin configuration in which both ordering momenta  $\mathbf{Q}_1$  or  $\mathbf{Q}_2$  are present. The stripe  $(0, \pi)$  or  $(\pi, 0)$  order is therefore preserved only if the interaction involving the second hole band is below the threshold and the second SDW order does not develop.

This in turn implies that, if the SDW order is  $(0, \pi)$  or  $(\pi, 0)$ , as the experiments indicate, only one hole and one electron FSs are involved in the SDW mixing. Other two bands (one hole band and one electron band) are not involved and remain the same as in the normal state. As a result, the system remain a metal for any coupling strength.

We argued that this peculiar requirement is related to the fact that both hole FSs are centered at  $(0,0)$ . If one of two hole FSs was instead centered at  $(\pi, \pi)$ , the second SDW order would have the same momentum as the first one (either  $\mathbf{Q}_1$  or  $\mathbf{Q}_2$ ) and the stripe order would survive. To illustrate this point, we considered a half-filled  $t$ - $t'$ - $U$  model in which the two hole bands are centered at  $(0,0)$  and  $(\pi, \pi)$ . In the

large  $U$  limit, the model reduces to  $J_1$ - $J_2$  model of localized spins. We argued that, in this model, the degeneracy of the found state SDW order-parameter manifold is not broken by either ellipticity or electron-electron interactions, and the degenerate manifold includes  $(0, \pi)$  and  $(\pi, 0)$  states even when all four bands are involved in the SDW mixing. The degeneracy is broken by fluctuations beyond mean field, which likely select the stripe order at any  $U$ . Because all four bands are involved, the stripe-ordered state in the  $t$ - $t'$ - $U$  model, it is a metal at small  $U$  and an insulator at large  $U$ .

We analyzed the electronic structure for parameters relevant to the pnictides, for which SDW order is moderate, and the two FSs involved in the SDW mixing are only partly gapped. We found three bands near  $k=(0,0)$  and three bands near  $k=(\pi, \pi)$  in the folded BZ, and more FS crossings than in the paramagnetic state. We calculated ARPES intensity and found a number of features consistent with the data. In particular, we found “Dirac points” in the dispersion near  $(0,0)$  and an electron band and two hole “half bands” (hole “blades”) near  $(\pi, \pi)$ .

We believe that the good agreement with ARPES experiments is a strong argument in favor of the itinerant scenario for the ferropnictides. We emphasize that the itinerant scenario does not imply that the system must be in a weak-coupling regime. Interactions in the pnictides are moderately strong and, quite possibly, give rise to some redistribution of the spectral weight up to high energies.<sup>9,24,42</sup> The only requirement for the applicability of our itinerant approach is the existence of a substantial spectral weight at low energies, where the system behaves as an interacting Fermi liquid.

## ACKNOWLEDGMENTS

We thank E. Abrahams, W. Brenig, S. Borisenko, P. Brydon, D. Evtushinsky, A. Kordyuk, J. Knolle, I. Mazin, Q. Si, O. Sushkov, N. Shannon, Z. Tesanovic, C. Timm, M. Vavilov, A. Vorontsov, G. Uhrig, and V. B. Zabolotnyy for useful discussions. We are particularly thankful to Z. Tesanovic for detecting an error in the early version of the paper. I.E. acknowledges the support from the RMES Program (Contract No. N 2.1.1/3199), NSF (Grant No. DMR-0456669), and thanks for hospitality UW Madison where this work was initiated. A.V.C. acknowledges the support from NSF under Grant No. DMR-0906953, MPI PKS in Dresden, and Aspen Center for Theoretical Physics, where this work has been completed.

\*On leave from Physics Department, Kazan State University, 420008 Kazan, Russia

<sup>1</sup>Y. Kamihara, T. Watanabe, M. Hirano, and H. Hosono, J. Am. Chem. Soc. **130**, 3296 (2008).

<sup>2</sup>I. I. Mazin, D. J. Singh, M. D. Johannes, and M. H. Du, Phys. Rev. Lett. **101**, 057003 (2008); K. Kuroki, S. Onari, R. Arita, H. Usui, Y. Tanaka, H. Kontani, and H. Aoki, *ibid.* **101**, 087004 (2008); V. Barzykin and L. P. Gorkov, JETP Lett. **88**, 142 (2008).

<sup>3</sup>T. A. Maier, S. Graser, D. J. Scalapino, and P. J. Hirschfeld, Phys. Rev. B **79**, 224510 (2009); A. V. Chubukov, M. G. Vavilov, and A. B. Vorontsov, *ibid.* **80**, 140515(R) (2009); R. Thomale, C. Platt, J. Hu, C. Honerkamp, and B. A. Bernevig, *ibid.* **80**, 180505 (2009).

<sup>4</sup>D. V. Evtushinsky, D. S. Inosov, V. B. Zabolotnyy, A. Koitzsch, M. Knupfer, B. Büchner, M. S. Viazovska, G. L. Sun, V. Hinkov, A. V. Boris, C. T. Lin, B. Keimer, A. Varykhalov, A. A. Kordyuk, and S. V. Borisenko, Phys. Rev. B **79**, 054517 (2009);

- D. Hsieh, Y. Xia, L. Wray, D. Qian, K. Gomes, A. Yazdani, G. F. Chen, J. L. Luo, N. L. Wang, and M. Z. Hasan, arXiv:0812.2289 (unpublished).
- <sup>5</sup>A. I. Coldea, J. D. Fletcher, A. Carrington, J. G. Analytis, A. F. Bangura, J.-H. Chu, A. S. Erickson, I. R. Fisher, N. E. Hussey, and R. D. McDonald, Phys. Rev. Lett. **101**, 216402 (2008).
  - <sup>6</sup>Clarina de la Cruz, Q. Huang, J. W. Lynn, J. Li, W. Ratcliff II, J. L. Zarestky, H. A. Mook, G. F. Chen, J. L. Luo, N. L. Wang, and P. Dai, Nature (London) **453**, 899 (2008).
  - <sup>7</sup>H.-H. Klauss, H. Luetkens, R. Klingeler, C. Hess, F. J. Litterst, M. Kraken, M. M. Korshunov, I. Eremin, S.-L. Drechsler, R. Khasanov, A. Amato, J. Hamann-Borrero, N. Leps, A. Kondrat, G. Behr, J. Werner, and B. Büchner, Phys. Rev. Lett. **101**, 077005 (2008).
  - <sup>8</sup>P. Chandra, P. Coleman, and A. I. Larkin, Phys. Rev. Lett. **64**, 88 (1990).
  - <sup>9</sup>Q. Si and E. Abrahams, Phys. Rev. Lett. **101**, 076401 (2008); C. Fang, H. Yao, W.-F. Tsai, J. P. Hu, and S. A. Kivelson, Phys. Rev. B **77**, 224509 (2008); Cenke Xu, Markus Muller, and Subir Sachdev, *ibid.* **78**, 020501(R) (2008); T. Yildirim, Phys. Rev. Lett. **101**, 057010 (2008); Goetz S. Uhrig, Michael Holt, Jaan Oitmaa, Oleg P. Sushkov, and Rajiv R. P. Singh, Phys. Rev. B **79**, 092416 (2009).
  - <sup>10</sup>V. Cvetkovic and Z. Tesanovic, EPL **85**, 37002 (2009); see also V. Stanev, J. Kang, and Z. Tesanovic, Phys. Rev. B **78**, 184509 (2008).
  - <sup>11</sup>V. Barzykin and L. P. Gorkov, JETP Lett. **88**, 131 (2008).
  - <sup>12</sup>A. V. Chubukov, D. V. Efremov, and I. Eremin, Phys. Rev. B **78**, 134512 (2008); A. V. Chubukov, Physica C **469**, 640 (2009).
  - <sup>13</sup>F. Wang, H. Zhai, Y. Ran, A. Vishwanath, and D.-H. Lee, Phys. Rev. Lett. **102**, 047005 (2009).
  - <sup>14</sup>M. M. Korshunov and I. Eremin, Phys. Rev. B **78**, 140509(R) (2008); EPL **83**, 67003 (2008).
  - <sup>15</sup>P. M. R. Brydon and C. Timm, Phys. Rev. B **79**, 180504(R) (2009).
  - <sup>16</sup>M. D. Johannes and I. I. Mazin, Phys. Rev. B **79**, 220510(R) (2009); see also I. I. Mazin and M. D. Johannes, Nat. Phys. **5**, 141 (2009).
  - <sup>17</sup>C. Platt, C. Honerkamp, and W. Hanke, New J. Phys. **11**, 055058 (2009).
  - <sup>18</sup>M. T. Rice, Phys. Rev. B **2**, 3619 (1970); N. Kulikov and V. V. Tugushev, Sov. Phys. Usp. **27**, 954 (1984) [Usp. Fiz. Nauk **144** 643 (1984)] and references therein see also L. V. Keldysh and Yu. V. Kopaev, Sov. Phys. Solid State **6**, 2219 (1965); J. De Cloizeaux, J. Phys. Chem. Solids **26**, 259 (1965); B. I. Halperin and M. T. Rice, Solid State Phys. **21**, 125 (1968).
  - <sup>19</sup>D. J. Singh and M.-H. Du, Phys. Rev. Lett. **100**, 237003 (2008); L. Boeri, O. V. Dolgov, and A. A. Golubov, *ibid.* **101**, 026403 (2008).
  - <sup>20</sup>D. H. Lu, M. Yi, S.-K. Mo, A. S. Erickson, J. Analytis, J.-H. Chu, D. J. Singh, Z. Hussain, T. H. Geballe, I. R. Fisher, and Z.-X. Shen, Nature (London) **455**, 81 (2008).
  - <sup>21</sup>C. Liu, T. Kondo, M. E. Tillman, R. Gordon, G. D. Samolyuk, Y. Lee, C. Martin, J. L. McChesney, S. Bud'ko, M. A. Tanatar, E. Rotenberg, P. C. Canfield, R. Prozorov, B. N. Harmon, and A. Kaminski, arXiv:0806.2147 (unpublished).
  - <sup>22</sup>C. Liu, G. D. Samolyuk, Y. Lee, N. Ni, T. Kondo, A. F. Santander-Syro, S. L. Bud'ko, J. L. McChesney, E. Rotenberg, T. Valla, A. V. Fedorov, P. C. Canfield, B. N. Harmon, and A. Kaminski, Phys. Rev. Lett. **101**, 177005 (2008).
  - <sup>23</sup>H. Ding, K. Nakayama, P. Richard, S. Souma, T. Sato, T. Takahashi, M. Neupane, Y.-M. Xu, Z.-H. Pan, A. V. Fedorov, Z. Wang, X. Dai, Z. Fang, G. F. Chen, J. L. Luo, and N. L. Wang, arXiv:0812.0534 (unpublished).
  - <sup>24</sup>S. J. Moon, J. H. Shin, D. Parker, W. S. Choi, I. I. Mazin, Y. S. Lee, J. Y. Kim, N. H. Sung, B. K. Cho, S. H. Khim, J. S. Kim, K. H. Kim, and T. W. Noh, arXiv:0909.3352 (unpublished).
  - <sup>25</sup>Takeshi Kondo, R. M. Fernandes, R. Khasanov, Chang Liu, A. D. Palczewski, Ni Ni, M. Shi, A. Bostwick, E. Rotenberg, J. Schmalian, S. L. Bud'ko, P. C. Canfield, and A. Kaminski, arXiv:0905.0271 (unpublished).
  - <sup>26</sup>G. Liu, H. Liu, L. Zhao, W. Zhang, X. Jia, J. Meng, X. Dong, J. Zhang, G. F. Chen, G. Wang, Y. Zhou, Y. Zhu, X. Wang, Z. Xu, C. Chen, and X. J. Zhou, Phys. Rev. B **80**, 134519 (2009).
  - <sup>27</sup>V. B. Zabolotnyy, D. S. Inosov, D. V. Evtushinsky, A. Koitzsch, A. A. Kordyuk, G. L. Sun, J. T. Park, D. Haug, V. Hinkov, A. V. Boris, C. T. Lin, M. Knupfer, A. N. Yaresko, B. Buechner, A. Varykhalov, R. Follath, and S. V. Borisenko, Nature (London) **457**, 569 (2009).
  - <sup>28</sup>M. Yi, D. H. Lu, J. G. Analytis, J.-H. Chu, S.-K. Mo, R.-H. He, M. Hashimoto, R. G. Moore, I. I. Mazin, D. J. Singh, Z. Hussain, I. R. Fisher, and Z.-X. Shen, Phys. Rev. B **80**, 174510 (2009).
  - <sup>29</sup>A. I. Coldea, C. M. J. Andrew, J. G. Analytis, R. D. McDonald, A. F. Bangura, J.-H. Chu, I. R. Fisher, and A. Carrington, Phys. Rev. Lett. **103**, 026404 (2009).
  - <sup>30</sup>Y. Xia, D. Qian, L. Wray, D. Hsieh, G. F. Chen, J. L. Luo, N. L. Wang, and M. Z. Hasan, Phys. Rev. Lett. **103**, 037002 (2009).
  - <sup>31</sup>V. Cvetkovic and Z. Tesanovic (unpublished); Z. Tesanovic (private communication).
  - <sup>32</sup>V. Barzykin and L. P. Gor'kov, Phys. Rev. B **79**, 134510 (2009).
  - <sup>33</sup>D. Parker, M. G. Vavilov, A. V. Chubukov, I. I. Mazin, Phys. Rev. B **80**, 100508(R) (2009).
  - <sup>34</sup>J. R. Schrieffer, X. G. Wen, and S. C. Zhang, Phys. Rev. B **39**, 11663 (1989); A. Singh and Z. Tesanovic, *ibid.* **41**, 614 (1990); A. V. Chubukov and D. M. Frenkel, *ibid.* **46**, 11884 (1992).
  - <sup>35</sup>Y. Ran, F. Wang, H. Zhai, A. Vishwanath, and D.-H. Lee, Phys. Rev. B **79**, 014505 (2009).
  - <sup>36</sup>A. B. Vorontsov, M. G. Vavilov, A. V. Chubukov, Phys. Rev. B **79**, 060508(R) (2009).
  - <sup>37</sup>P. M. R. Brydon and C. Timm, Phys. Rev. B **80**, 174401 (2009).
  - <sup>38</sup>E. Kaneshita, T. Morinari, and T. Tohyama, Phys. Rev. Lett. **103**, 247202 (2009).
  - <sup>39</sup>J. Lorenzana, G. Seibold, C. Ortix, and M. Grilli, Phys. Rev. Lett. **101**, 186402 (2008).
  - <sup>40</sup>P. Richard, K. Nakayama, T. Sato, M. Neupane, Y.-M. Xu, J. H. Bowen, G. F. Chen, J. L. Luo, N. L. Wang, H. Ding, and T. Takahashi, arXiv:0909.0574 (unpublished).
  - <sup>41</sup>N. Harrison and S. E. Sebastian, arXiv:0910.4199 (unpublished).
  - <sup>42</sup>A. Georges, G. Kotliar, W. Krauth, and M. J. Rozenberg, Rev. Mod. Phys. **68**, 13 (1996).